Check for updates

Accepted Article

Triboelectric Nanogenerators Based on Fluid Medium: From Fundamental Mechanisms toward Multifunctional Applications

*Feng Jiang, Liuxiang Zhan, Jin Pyo Lee and Pooi See Lee**

F. Jiang

Institute of Flexible Electronics Technology of Tsinghua, Jiaxing, Zhejiang 314000, China

F. Jiang, L. X. Zhan, Dr. J. P. Lee, Prof. P. S. Lee

School of Materials Science and Engineering, Nanyang Technological University, 50 Nanyang Avenue, Singapore 639798, Singapore

E-mail: pslee@ntu.edu.sg

Keywords: fluids, triboelectric nanogenerators, energy harvesters, interfaces, charge transfer

Abstract

Fluid-based triboelectric nanogenerators (FB-TENGs) are at the forefront of promising energy technologies, demonstrating the ability to generate electricity through the dynamic interaction between two dissimilar materials, wherein at least one is a fluidic medium (such as gas or liquid). By capitalizing on the dynamic and continuous properties of fluids and their interface interactions, FB-TENGs exhibit a larger effective contact area and a longer-lasting triboelectric effect in comparison to their solid-based counterparts, thereby affording longer-term energy harvesting and higher-

This article has been accepted for publication and undergone full peer review but has not been through the copyediting, typesetting, pagination and proofreading process, which may lead to differences between this version and the Version of Record. Please cite this article as doi: 10.1002/adma.202308197.

This article is protected by copyright. All rights reserved.

Accepted Article

precision self-powered sensors in harsh conditions. In this review, various fluid-based mechanical energy harvesters, including liquid-solid, gas-solid, liquid-liquid and gas-liquid TENGs, have been systematically summarized. Their working mechanism, optimization strategies, respective advantages and applications, theoretical and simulation analysis, as well as the existing challenges, have also been comprehensively discussed, which provide prospective directions for device design and mechanism understanding of FB-TENGs.

1. Introduction

Triboelectric nanogenerator (TENG), serving as a clean and sustainable energy technology, enables a direct energy conversion from disordered high-entropy mechanical energy into electricity based on the coupling effect of contact electrification and electrostatic induction. The past decade has witnessed a giant boom in TENG development varying from theoretical framework construction to material innovation and structure optimization, giving rise to an abundance of practical applications in soft robotics, biomedical sensors, environmental purification and smart haptics.[1-4] Despite the marvelous progress, most efforts were still focused on solid-solid TENGs on account of their simple structure design and device fabrication. Nevertheless, the intrinsically unavoidable wear issue and high environmental sensitivity (*e.g.* humidity and atmospheric pressure) at solid surfaces set severe restrictions on the durability and stability of solid-solid TENGs, impeding their further applications in long-term power supply and high-precision self-powered sensors.

By contrast to traditional solid-solid TENGs, fluid-based triboelectric nanogenerators (FB-TENGs) generate electricity via the interaction between a fluidic medium (*e.g.* gas or liquid) and a solid material (or another fluidic medium). The dynamic nature of fluid offers a consistent, stable and soft

This article is protected by copyright. All rights reserved.

15214095, ja, Downloaded from https://onlinelibrary.wiley.com/doi/10.1002/adma.202308197 by Nanyang Technological University Lee Kong Chian School Of Medicine, Wiley Online Library on [16/10/2023]. See the Terms and Conditions (https://onlinelibrary.wiley.com/terms-and-conditions) on Wiley Online Library for rules of use; OA articles are governed by the applicable Creative Commons License

Accepted Article

contact at the interface, rendering FB-TENG to sustain a longer triboelectric effect and stronger wear resistance. Meanwhile, the fluid also provides a larger contact area owing to its inherent fluidity and conformability to various materials or structures, which not only promotes charge transfer and energy conversion efficiency, but also enables its integration with other flexible and stretchable materials. Furthermore, FB-TENG affords more versatile energy harvesting possibilities compared to solid-solid TENGs. For example, it can efficiently capture mechanical energy from various forms of flowing substances, encompassing liquids (e.g. raindrops, water currents and biological fluids) and gases (e.g. breeze and wind), and then convert it into electricity, exhibiting its tremendous potential in blue energy, environmental monitoring and biomedical sensors.

In this review, we systematically summarize the fundamentals and state-of-art progress of FB-TENGs, which mainly concentrate on liquid-solid TENG, gas-solid TENG, liquid-liquid TENG and gas-liquid TENG. Some revolutionary progresses that advanced this field have been also highlighted in **Figure 1**. Although some existing reviews were referring to FB-TENGs[5-7], the focus was mainly concentrated on their mechanism and applications, while a methodological guidance or optimization strategy to design high-performance FB-TENGs is still lacking. On the other hand, a systematic analysis based on a theoretical or simulation model is also of interest in this area, which is the foundation to reveal the working mechanism and the bedrock to design high-performance FB-TENGs. Herein, a more comprehensive discussion, including the working mechanism, theoretical and simulation analysis, optimization strategies and respective advantages of various FB-TENGs, is provided, which can serve as a guideline for high-performance device design from the aspects of material engineering and structural architecture. Related to this, we also demonstrate the fascinating applications of diverse FB-TENGs ranging from implantable biomonitoring sensors to

This article is protected by copyright. All rights reserved.

15214095, ja, Downloaded from https://onlinelibrary.wiley.com/doi/10.1002/adma.202308197 by Nanyang Technological University Lee Kong Chian School Of Medicine, Wiley Online Library on [16/10/2023]. See the Terms and Conditions (https://onlinelibrary.wiley.com/terms-and-conditions) on Wiley Online Library for rules of use; OA articles are governed by the applicable Creative Commons License

large-scale and distributed power systems. Finally, we highlight the scientific challenges and promising perspectives existing in this emerging field, primarily focusing on the requirements for new theoretical model construction and broader application exploration.

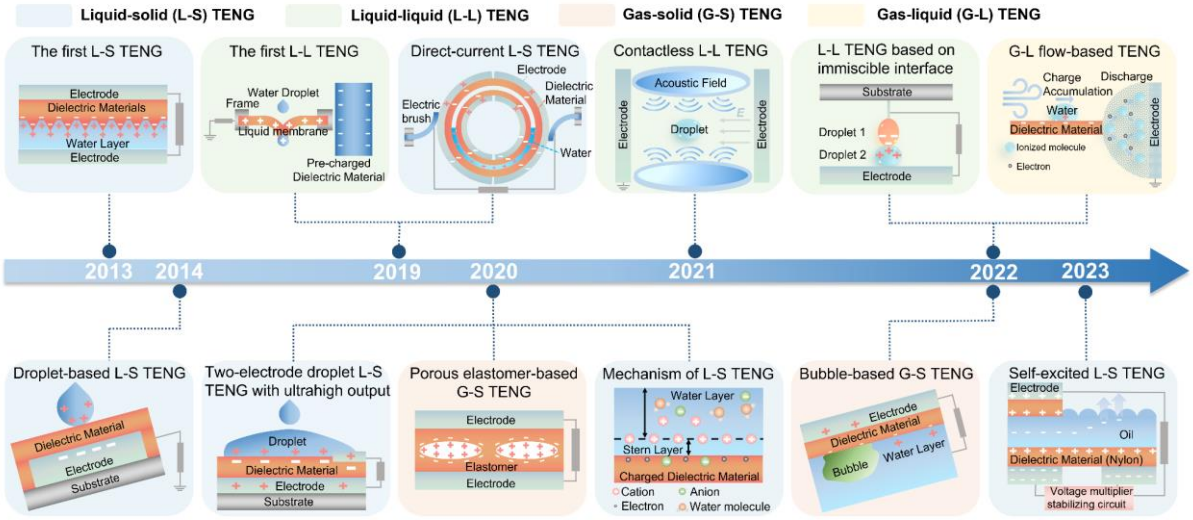

Figure 1. Timeline of significant advancements in fluid-based triboelectric nanogenerator. The first liquid-solid TENG based on the contact electrification between the water layer and dielectric material. Reproduced with permission.[8] Copyright 2013, Wiley-VCH. A water droplet-based TENG with superhydrophobic and self-cleaning characteristics for harvesting water energy. Reproduced with permission.[9] Copyright 2014, Wiley-VCH. The first liquid-liquid TENG based on a freely suspended liquid membrane. Reproduced with permission.[10] Copyright 2019, Springer Nature. The rotary-tubular structure with direct-current outputs. Reproduced with permission.[11] Copyright 2019, American Chemical Society. A two-electrode droplet-based liquid-solid TENG with high instantaneous power density (50 W m^{-2}). Reproduced with permission.[12] Copyright 2020, Springer Nature. A porous elastomer with closed voids for harvesting the mechanical energy from gas-solid interaction. Reproduced with permission.[13] Copyright 2020, AAAS. A contact electrification model in combination with an electric double layer model for the mechanism understanding at the liquid-solid interface. Reproduced with permission.[14] Copyright 2020, Springer Nature. A contactless liquid-

This article is protected by copyright. All rights reserved.

Accepted Article

15214095, ja, Downloaded from https://onlinelibrary.wiley.com/doi/10.1002/adma.202308197 by Nanyang Technological University Lee Kong Chian School Of Medicine, Wiley Online Library on [16/10/2023]. See the Terms and Conditions (https://onlinelibrary.wiley.com/terms-and-conditions) on Wiley Online Library for rules of use; OA articles are governed by the applicable Creative Commons License

liquid electrification TENG based on the combination of electric field and acoustic field. Reproduced with permission.[15] Copyright 2021, Wiley-VCH. An immiscible liquid-liquid interface for efficient charge transfer between two aqueous interfaces. Reproduced with permission.[16] Copyright 2022, Springer Nature. The gas-liquid two-phase flow platform with an ultrahigh output power (144 kW m^{-3}). Reproduced with permission.[17] Copyright 2022, AAAS. A transistor-inspired bubble energy generator, with tailored surface wettability and two-electrode design. Reproduced with permission.[18] Copyright 2022, AAAS. Self-excited liquid suspension system with optimized charge transportation displaying excellent durability (234 k operating cycles) and high charge density (704 μC m^{-2}). Reproduced with permission.[19] Copyright 2023, Wiley-VCH.

2. Liquid-Solid TENG

Since the inception of triboelectric nanogenerators[20], significant attention has been directed toward the development of all-solid-based device designs, owing to their operational convenience and facile fabrication. Nevertheless, traditional solid-solid TENGs have encountered numerous inevitable challenges, including high environmental sensitivity (especially concerning humidity and atmospheric pressure), wear and abrasion resulting from continuous collision and friction, and limited contact area for effective electrification.[21-22] In view of these issues, liquid-solid TENGs have emerged as promising solutions, benefiting from the uniquely dynamic, fluidity and conformability of liquids, as well as the soft contact between the liquid and solid materials.[23-28] While various liquid-solid TENGs with diverse operation modes and device structures have been demonstrated, they can principally be categorized into two types: droplet-based and liquid flow/wave-based systems.

2.1 Mechanism

The operational mechanism underlying liquid-solid TENGs stems from a synergy of the contact electrification between liquids and solids and the electrostatic screening effect. A significant point to

This article is protected by copyright. All rights reserved.

Accepted Article

15214095, ja, Downloaded from https://onlinelibrary.wiley.com/doi/10.1002/adma.202308197 by Nanyang Technological University Lee Kong Chian School Of Medicine, Wiley Online Library on [16/10/2023]. See the Terms and Conditions (https://onlinelibrary.wiley.com/terms-and-conditions) on Wiley Online Library for rules of use; OA articles are governed by the applicable Creative Commons License

Accepted Article

achieve continuous electrification is to construct a stable and dynamic liquid-solid interface. Considering the distinct forms of moving liquids within the system, they can be categorized into two primary types: continuous and discontinuous mediums. This classification has, in turn, given rise to the development of two major operational modes, namely, droplet-based liquid-solid TENGs and liquid flow/wave-based liquid-solid TENGs.

2.1.1. Mechanism of Droplet-Based Liquid-Solid TENG

Liquid droplets have been considered as energy carriers as they contain kinetic energy converted from potential energy as well as electrostatic energy generated by contact electrification with air particles. By utilizing the electrostatic energy stored inside the water droplets, Wang et al. proposed a sequential contact-electrification and electrostatic induction process to achieve dynamic interactions between the water droplets and the solid surface.[9] The working mechanism of this liquid-solid TENG is illustrated in **Figure 2**a. When the water droplet contacts a polymer film, the ionization of surface groups will induce negative charges to the polymers, while the water droplet will be positively charged to maintain electrical neutrality. Owing to the dielectric properties and charge retention capacity of the polymer films, they can sustain the triboelectric negative charges for a longer time (Figure 2a (i)). Once the water droplet contacts with the negatively charged polymer film, the negative charges will attract counter ions from the water droplet to form an electric double layer (EDL), establishing a positive electric potential difference. Therefore, electrons will flow via an external circuit (Figure 2a (ii)) until an equilibrium is achieved (Figure 2a (iii)). This process produces an instantaneous positive current. As the water droplet leaves the surface of the polymer, a negative electric potential difference will be introduced between the electrode and ground, so electrons will transfer from the electrode to the ground until a new equilibrium is

This article is protected by copyright. All rights reserved.

15214095, ja, Downloaded from https://onlinelibrary.wiley.com/doi/10.1002/adma.202308197 by Nanyang Technological University Lee Kong Chian School Of Medicine, Wiley Online Library on [16/10/2023]. See the Terms and Conditions (https://onlinelibrary.wiley.com/terms-and-conditions) on Wiley Online Library for rules of use; OA articles are governed by the applicable Creative Commons License

established (Figure 2a (iv)). With this periodic interaction between the water droplets and the polymer film, a continuous alternating current output will be generated. By virtue of this dynamic interaction between falling water droplets and solids, the mechanical energy can be effectively harvested from the raindrops, offering a promising approach to quantitatively investigate the charge transfer behaviors at the liquid-solid interface.

2.1.2. Mechanism of Flow/Wave-Based Liquid-Solid TENG

In contrast to droplets, the continuous liquid impact in the form of streaming flow or water waves has been investigated as a viable hydropower source, enabling energy harvesting from various water sources, such as pipe flows, running waters, rivers, and water waves. Conventionally, electromagnetic generators were employed for wave energy harvesting, but their practical applications were hindered by their high-cost fabrication and maintenance due to their bulky volume and substantial weight.[29] Accordingly, flow/wave-based liquid-solid TENGs have been developed to collect energy from various water motions through liquid-solid electrification and electrostatic induction.[30-32] The working mechanism of the flow/wave-based liquid-solid TENG is demonstrated in Figure 2b. Analogous to droplet-based liquid-solid TENG, the negative charges will be first introduced and sustained at the surface of the polymer film (Figure 2b (i)). Upon partial submersion of the device due to rising water levels, certain positive charges present in the water (*e.g.* hydronium ion) will partially screen the negative charges at the surface of the polymer film by forming an interfacial EDL (Figure 2b (ii)). This asymmetric distribution of charges will induce the unbalanced potential difference, driving free electrons to flow via the external circuit until the device is fully submerged and triboelectric charges are entirely screened (Figure 2b (iii)). As the water wave recedes, electrons will flow back in the opposite direction from the induction electrode

This article is protected by copyright. All rights reserved.

Accepted Article

15214095, ja, Downloaded from https://onlinelibrary.wiley.com/doi/10.1002/adma.202308197 by Nanyang Technological University Lee Kong Chian School Of Medicine, Wiley Online Library on [16/10/2023]. See the Terms and Conditions (https://onlinelibrary.wiley.com/terms-and-conditions) on Wiley Online Library for rules of use; OA articles are governed by the applicable Creative Commons License

Accepted Article

to the ground until the device is fully emerged (Figure 2b (iv)). By controlling the movement of water flow/wave, continuous alternating current signals can be obtained, providing a practically feasible technology for blue energy harvesting.

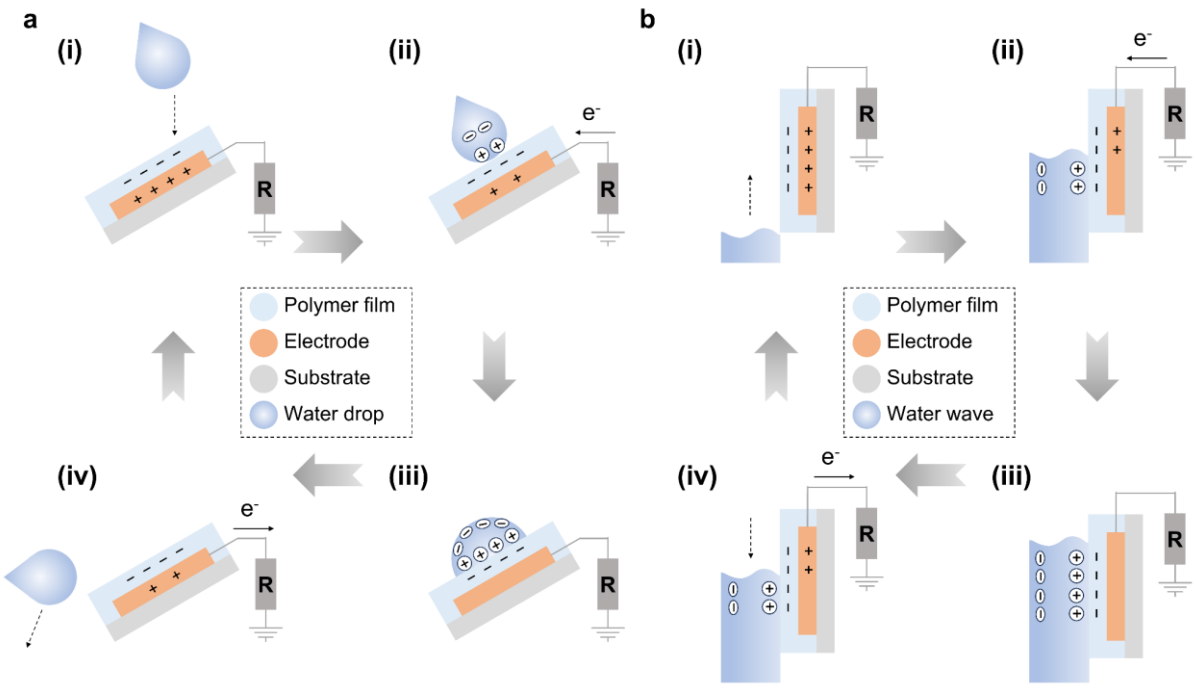

Figure 2. Working mechanism of liquid-solid TENGs. a) Working mechanism of droplet-based liquid-solid TENG. Reproduced with permission.[9] Copyright 2014, Wiley-VCH. b) Working mechanism of liquid flow/wave-based liquid-solid TENG. Reproduced with permission.[30] Copyright 2014, American Chemical Society.

2.2. Optimization Strategies

Optimization strategies for liquid-solid TENGs primarily revolve around two key aspects: materials modification and structural design. In the context of material considerations related to the liquid component, physicochemical properties such as ionic activity, pH and polarity, are considered as

This article is protected by copyright. All rights reserved.

15214095, ja, Downloaded from https://onlinelibrary.wiley.com/doi/10.1002/adma.202308197 by Nanyang Technological University Lee Kong Chian School Of Medicine, Wiley Online Library on [16/10/2023]. See the Terms and Conditions (https://onlinelibrary.wiley.com/terms-and-conditions) on Wiley Online Library for rules of use; OA articles are governed by the applicable Creative Commons License

Accepted Article

important factors that affect the charge transfer between the liquid and solid. On the other hand, for solid materials, the focus lies on achieving superhydrophobic and nanostructured surfaces through surface modification and functionalization. This serves to enhance both contact-separation efficiency and the effective surface area available for energy conversion. Furthermore, a multitude of structural design approaches are introduced with the aim of establishing highly efficient and conformal contact between the liquid and solid mediums. These innovative designs encompass optimizations to the solid surface and adjustments to electrode configurations. This section will provide a comprehensive overview of the aforementioned optimization strategies, offering prospective strategies for high-performance liquid-solid TENG design.

Expanding the range of materials from solids to liquids has opened up new avenues for performance enhancement considering the unique properties of liquids. To elucidate the correlation between electric output performance and various liquid characteristics (*e.g.* ionic activity, pH, and polarity), Nie et al. investigated the charge transfer process between an aqueous solution and a polytetrafluoroethylene (PTFE) film by varying the ion concentration and pH values, as depicted in **Figure 3**a.[33-34] From the results, the number of transferred charges would reach the maximum when the NaCl concentration was ~1×10^{-5} mol L^{-1} and pH was distributed between 5 and 9 (Figure 3a (i)). It was found that a slight increase in ion concentration could promote charge transfer, but the further increment of the ion concentration would cause excessive ion accumulation in the liquid solution, which hindered the electron transfer process due to the screening effect. Meanwhile, the solution with high H^+ concentration exhibited a negative charge once separated from its contact with PTFE (Figure 3a (i)). This intriguing phenomenon arose from the competition between H^+ adsorption and electron transfer where a substantial concentration of H^+ ions would be adsorbed on the surface

This article is protected by copyright. All rights reserved.

15214095, ja, Downloaded from https://onlinelibrary.wiley.com/doi/10.1002/adma.202308197 by Nanyang Technological University Lee Kong Chian School Of Medicine, Wiley Online Library on [16/10/2023]. See the Terms and Conditions (https://onlinelibrary.wiley.com/terms-and-conditions) on Wiley Online Library for rules of use; OA articles are governed by the applicable Creative Commons License

Accepted Article

of PTFE after the separation process, restraining the following electron transfer between the water molecules and the PTFE material. The tribo-polarity effect was also explored to understand the contact electrification mechanism at diverse water/polymer interfaces by combining the density functional theory and charge transfer measurements (Figure 3a (ii)). The results indicated that the electron transfer only occurred at the outmost atomic layer of the water/polymer interface where the atomic types and locations (*e.g.* parallel or vertical ordering) had a crucial impact on the contact electrification between the liquid and solid.

The material and structure optimization for solid materials are also significant to attain superior performance in liquid-solid TENGs (Figure 3b).[35-41] Polydimethylsiloxane (PDMS), fluorinated ethylene propylene (FEP), polyethylene terephthalate (PET) and PTFE, possessing both excellent hydrophobicity and tribo-negative properties, have been widely utilized as solid contact materials for liquid-solid TENGs. Various surface morphology designs inspired by biomimetic structures (*e.g.* Moth's eye and natural lotus leaf) were also prepared based on nano-/micro-engineering fabrication (Figure 3b (i)), which not only achieved a superhydrophobic surface, but also promoted a better charge transfer and surface charge density on account of the increased contact-separation efficiency and specific surface area. Surface modification is another strategy to endow solid materials with superhydrophobicity and high surface charge density. As demonstrated in Figure 3b (ii), the electric performance of the device can be substantially enhanced by tuning the surface functional groups from electron-donating group (*e.g.* -NH_2) to electron-withdrawing group (*e.g.* -CF_3), offering a controllable approach for the utilization or the prevention of solid–liquid friction charges.

This article is protected by copyright. All rights reserved.

15214095, ja, Downloaded from https://onlinelibrary.wiley.com/doi/10.1002/adma.202308197 by Nanyang Technological University Lee Kong Chian School Of Medicine, Wiley Online Library on [16/10/2023]. See the Terms and Conditions (https://onlinelibrary.wiley.com/terms-and-conditions) on Wiley Online Library for rules of use; OA articles are governed by the applicable Creative Commons License

Accepted Article

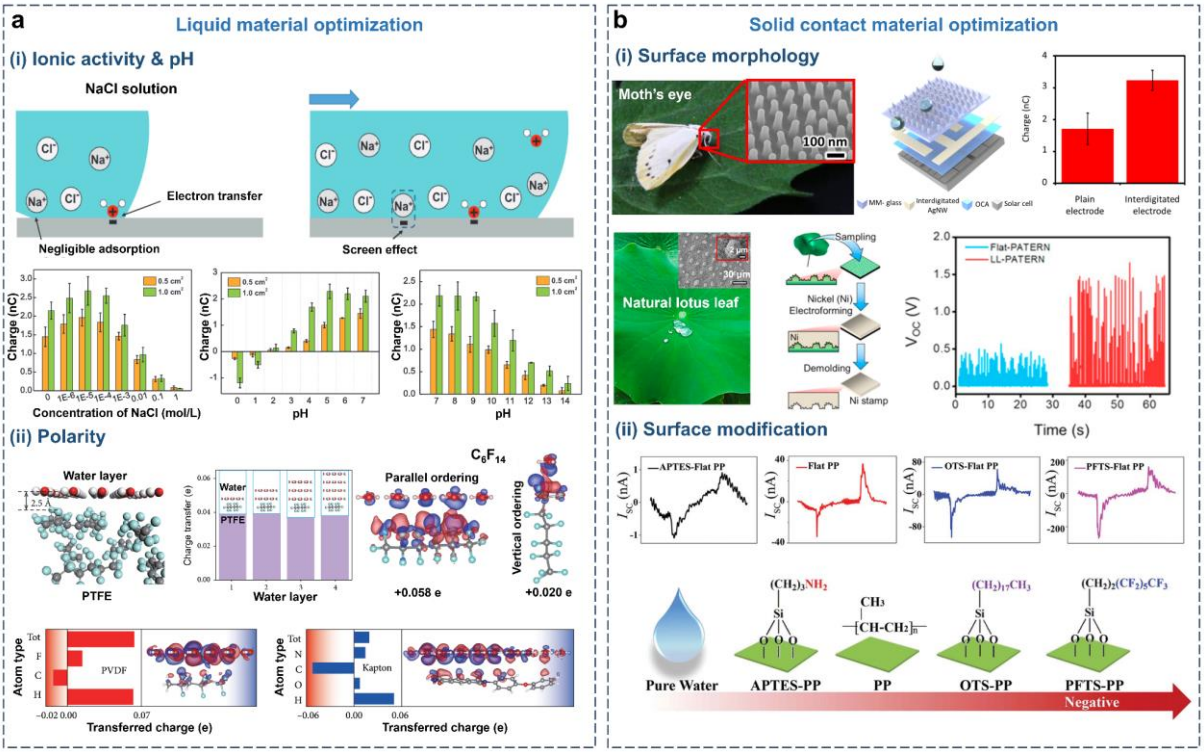

Figure 3. Optimization strategies for liquid-solid TENGs. a) Charge transfer between aqueous solution and PTFE film under different ion concentrations and pH values (a-i). Reproduced with permission.[33] Copyright 2020, Wiley-VCH. Schematic of the DFT simulation model and charge transfer measurements under a different number of water layers, atomic locations (*e.g.* parallel or vertical ordering) as well as the atomic composition for various polymers (*e.g.* PTFE, PVDF and Kapton) (a-ii). Reproduced with permission.[34] Copyright 2022, AAAS. b) Various surface morphologies for superhydrophobic property and high surface charge density inspired by biomimetic structures such as the moth's eye and lotus leaf (b-i). (top) Reproduced with permission.[36] Copyright 2019, Elsevier. (bottom) Reproduced with permission.[37] Copyright 2017, Elsevier. Surface modification techniques for high electric outputs based on tailoring different functional groups (b-ii). Reproduced with permission.[39] Copyright 2019 Wiley-VCH.

2.2.1. Performance Optimization of Droplet-Based Liquid-Solid TENG

This article is protected by copyright. All rights reserved.

15214095, ja, Downloaded from https://onlinelibrary.wiley.com/doi/10.1002/adma.202308197 by Nanyang Technological University Lee Kong Chian School Of Medicine, Wiley Online Library on [16/10/2023]. See the Terms and Conditions (https://onlinelibrary.wiley.com/terms-and-conditions) on Wiley Online Library for rules of use; OA articles are governed by the applicable Creative Commons License

Accepted Article

In the realm of collision dynamics involving liquid droplets and solid surfaces, a systematic investigation has been conducted to discern the impact of various factors on output performance.[42-46] Specifically, the falling height of the droplet, the tilt angle of the solid surface, and the volume of the droplet have been methodically examined, aiming to enhance the overall efficiency and effectiveness of the electric output in this intriguing domain (**Figure 4**a).[37, 47-49] As displayed in Figure 4a (i), both the falling height of the droplet and the tilt angle of the solid surface would affect the electric outputs of the energy device. Notably, an augmented falling height facilitated an enhanced charge transfer between the droplet and solid, but an excessively increased falling height might lead to undesirable consequences, such as water splitting and rebounding of the droplets from the surface, which could hinder the charge transfer mechanism. On the other hand, there was also a trade-off between the electric output and tilted angle of the solid surface, as shown in Figure 4a (i). Particularly, the flow of the droplet was impeded at the solid surface when the contact angle was smaller than 45°, while the contact would become ineffective if the angle exceeded 45°, so an optimum output performance could be achieved when the contact angel was 45°. Furthermore, the output performance of the liquid-solid TENGs was also significantly influenced by the droplet volume. As depicted in Figure 4a (ii), a two-electrode droplet-based TENG was prepared to investigate the relationship between the output current and droplet volume.[49] From the results, a larger droplet volume enables a larger interfacial contact area and a stronger charge transfer process, resulting in a higher amplitude of output current.

Device design is another strategy for performance improvement of liquid-solid TENGs (Figure 4b).[12, 50-51] Peng et al. developed a droplet-based TENG with high output performance by introducing an arc-shape structure.[50] Compared to the inclined surface structure (I-TENG), this new

This article is protected by copyright. All rights reserved.

15214095, ja, Downloaded from https://onlinelibrary.wiley.com/doi/10.1002/adma.202308197 by Nanyang Technological University Lee Kong Chian School Of Medicine, Wiley Online Library on [16/10/2023]. See the Terms and Conditions (https://onlinelibrary.wiley.com/terms-and-conditions) on Wiley Online Library for rules of use; OA articles are governed by the applicable Creative Commons License

Accepted Article

arc-shaped surface structure (A-TENG) not only promoted an accelerated contact-separation speed and enhanced effective contact area, but also avoided the droplet splashing during the collision process at the liquid-solid interface, thereby facilitating the triboelectrification and charge generation process (Figure 4b (i)). As a result, the output current density has been improved by over one order of magnitude. In addition to the arc structure design, electrode configuration optimization is also significant to the performance improvement of droplet-based liquid-solid TENGs. As illustrated in Figure 4b (ii), a two-electrode device design, comprising of PTFE film, Al electrode, ITO electrode and water droplet, has been proposed for high-performance droplet-based TENG fabrication.[12] The performance of the conventional single-electrode device was significantly hampered by the presence of interfacial effects. However, the incorporation of an Al electrode brought about a crucial enhancement by facilitating directed and swift charge transfer between the two electrodes when the descending droplet made contact with the top Al electrode. This two-electrode configuration yielded remarkable results, with an impressive output voltage and current reaching 143.5 V and 270 μA, respectively. Notably, these values were approximately 300 and 2600 times greater than what could be achieved in the single-electrode mode. The significant enhancement in electrical performance can be elucidated from a circuit perspective. Specifically, PTFE and water droplet can be considered as the capacitor (C_p) and resistor (R_w), respectively. In the single-electrode mode, an interfacial capacitor (C_1) between the droplet and PTFE exists within the circuit, yet the entire system remains in an open-circuit state. Conversely, in the two-electrode design, another capacitor at the water/Al interface (C_2) forms within the circuit, converting the original open circuit into a closed one. In this scenario, the capacitance of C_p becomes negligible due to the greater thickness of the PTFE film in comparison to the EDL formed at the water/PTFE and

This article is protected by copyright. All rights reserved.

15214095, ja, Downloaded from https://onlinelibrary.wiley.com/doi/10.1002/adma.202308197 by Nanyang Technological University Lee Kong Chian School Of Medicine, Wiley Online Library on [16/10/2023]. See the Terms and Conditions (https://onlinelibrary.wiley.com/terms-and-conditions) on Wiley Online Library for rules of use; OA articles are governed by the applicable Creative Commons License

water/Al interfaces. Consequently, the voltage across C_p becomes several orders of magnitude higher than that across C_1 and C_2 when the droplet makes contact with the Al electrode. This phenomenon results in the generation of ultrahigh electric outputs.

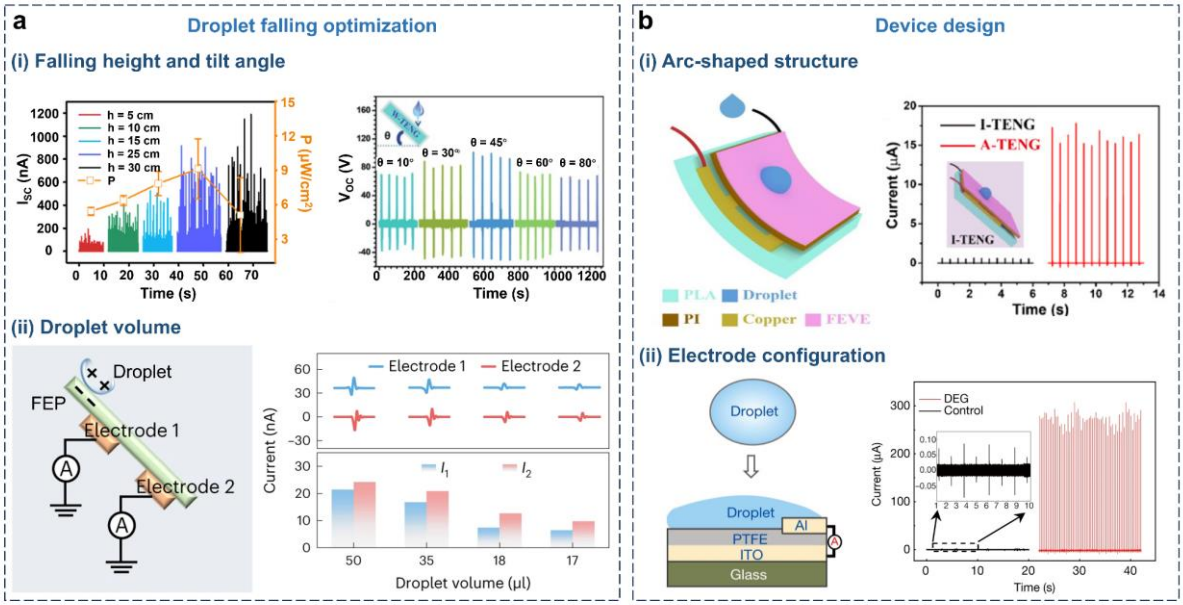

Figure 4. Optimization strategies of droplet-based liquid-solid TENGs. a) Effect of droplet falling height and the tilt angle of the solid surface on electric outputs of the TENGs (a-i). (left) Reproduced with permission.[37] Copyright 2017, Elsevier. (right) Reproduced with permission.[47] Copyright 2018, Wiley VCH. Relationship between the droplet volume and the electric outputs of TENG (a-ii). Reproduced with permission.[49] Copyright 2023, Springer Nature. b) Arc-shape structure with enhanced electric performance for a large effective contact-separation area under an accelerated contact-separation speed (b-i). Reproduced with permission.[50] Copyright 2022, Elsevier. Two-electrode configuration of droplet-based TENGs with high electric outputs. (b-ii). Reproduced with permission.[12] Copyright 2020, Springer Nature.

2.2.2. Performance Optimization of Water Flow/Wave-Based Liquid-Solid TENG

This article is protected by copyright. All rights reserved.

Accepted Article

15214095, ja, Downloaded from https://onlinelibrary.wiley.com/doi/10.1002/adma.202308197 by Nanyang Technological University Lee Kong Chian School Of Medicine, Wiley Online Library on [16/10/2023]. See the Terms and Conditions (https://onlinelibrary.wiley.com/terms-and-conditions) on Wiley Online Library for rules of use; OA articles are governed by the applicable Creative Commons License

Accepted Article

Similar to the droplet-based liquid-solid TENG, liquid flow/wave parameters, such as velocity and volume ratio, are also key factors to affect the triboelectric generation between liquid and solid surfaces (**Figure 5**a).[30, 52-53] As displayed in Figure 5a (i), the triboelectric output would increase with the increment of the velocity of water flow/wave because more dynamic interactions would be introduced at the interface between the liquid and solid, leading to higher surface charge densities and enhanced electrical outputs. The relationship between the water volume ratio and the output performance of the device was also investigated (Figure 5a (ii)). The findings revealed that low electric outputs were observed when the water volume ratio fell below 50%, primarily due to the inadequate water coverage at the PTFE surface, resulting in insufficient interfacial interactions. However, when the water volume ratio surpassed 50%, the output current experienced a sharp decline due to insufficient interfacial transition and irregular oscillation induced by water overflow. Consequently, the optimum electrical output was achieved at a 50% water volume ratio, a balance point that allowed for adequate surface coverage while avoiding excessive water overflow-induced irregularities.

Furthermore, various device structures have been also proposed to effectively capture the irregular mechanical energy from liquid flow/wave (Figure 5b).[11, 19, 38] For example, a direct current (DC) liquid-solid TENG has been developed based on the FEP tube and Cu electrode, as illustrated in Figure 5b (i). The liquid and Cu pellets, serving as fluidic dielectric materials, were prefilled within the ring-like FEP tube for charge generation. Two electric brushes were fixed at the two sides of the device to enable a stable charge flow direction by alternatively contacting the outer Cu electrodes, thereby resulting in a continuous DC output. In addition to the ring structure design, a self-excited liquid suspension TENG with a non-contact operation mode has been fabricated based on a

This article is protected by copyright. All rights reserved.

15214095, ja, Downloaded from https://onlinelibrary.wiley.com/doi/10.1002/adma.202308197 by Nanyang Technological University Lee Kong Chian School Of Medicine, Wiley Online Library on [16/10/2023]. See the Terms and Conditions (https://onlinelibrary.wiley.com/terms-and-conditions) on Wiley Online Library for rules of use; OA articles are governed by the applicable Creative Commons License

dielectric layer (nylon) and high-insulating liquid (silicone oil). As shown in Figure 5b (ii), triboelectric charges were firstly generated via the solid-liquid triboelectrification during the sliding process. Then the charges would be transported with the liquid flow and released to the ambient environment via the charge-liquid transmission and dissipation effect. Meanwhile, unbalanced charge density would be formed on the two triboelectric materials considering the different friction intensities for the slider and stator induced by liquid flow gradient, leading to the charge flow and power generation between the two bottom electrodes. Compared to traditional liquid-solid TENGs, this self-excited liquid suspension TENG combines the advantages of liquid interface lubrication, dual dielectric tribolayer design, charge space accumulation effect as well as the self-charge excitation circuit. Through this structure design, a high charge density of 704 μC m^{-2} and long durability of 234 k operating cycles could be achieved, setting a record among non-contact TENG devices, which provided a prospective strategy for robust and high-performance liquid-solid TENG design.

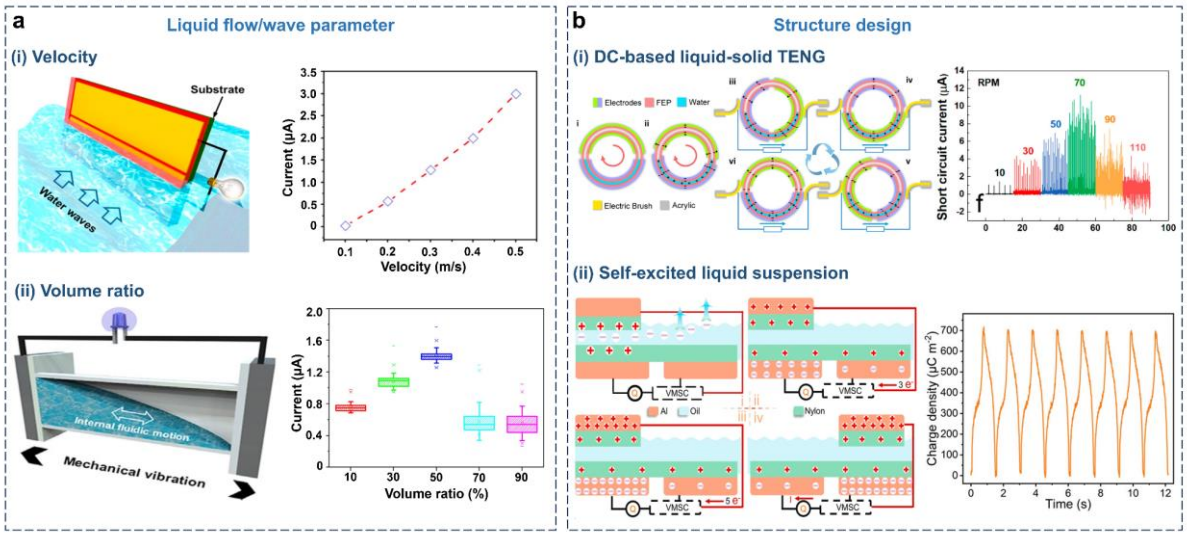

This article is protected by copyright. All rights reserved.

Accepted Article

15214095, ja, Downloaded from https://onlinelibrary.wiley.com/doi/10.1002/adma.202308197 by Nanyang Technological University Lee Kong Chian School Of Medicine, Wiley Online Library on [16/10/2023]. See the Terms and Conditions (https://onlinelibrary.wiley.com/terms-and-conditions) on Wiley Online Library for rules of use; OA articles are governed by the applicable Creative Commons License

Figure 5. Optimization strategies of liquid flow/wave-based TENGs. a) The influence of liquid flow/wave parameters such as (i) velocity and (ii) volume ratio on the output performance of liquid-solid TENGs. (a-i) Reproduced with permission.[30] Copyright 2014, American Chemical Society. (a-ii) Reproduced with permission.[53] Copyright 2017, Elsevier. b) The influence of device structure on the electric outputs of liquid flow/wave-based TENGs. (b-i) Mechanism of DC-based liquid-solid TENG and its corresponding current outputs under different rotation speeds. Reproduced with permission.[11] Copyright 2019, American Chemical Society. b-ii) Schematic diagrams of self-excited liquid suspension TENGs and the corresponding charge density during the working process. Reproduced with permission.[19] Copyright 2023, Wiley-VCH.

2.3. Advantages and Possible Applications of Liquid-Solid TENGs

By combining the dynamic and continuous nature of liquid mediums, liquid-solid TENGs provide a host of advantages over their solid-solid counterparts. For instance, the incorporation of a liquid medium offers a protective layer for solid contact material, which can reduce abrasion and promote the prolonged durability of the TENG device. This advantage not only extends the operation lifetime of the device but also ensures stable output performance under harsh conditions (*e.g.* high humidity environment). Liquid-solid TENGs also exhibited their potential in biosensors and chemical detection in liquid. Since the output performance of the liquid-solid TENGs is highly correlated with the molecules adsorbed on the surface of the solid component, the device can function as an efficient self-powered chemical sensor enabling the continuous monitoring of target chemical quantities.[54] As illustrated in **Figure 6**a (i), a novel self-powered biochemical sensor has been successfully fabricated, employing a combination of PTFE film and Cu electrode. This innovative sensor design demonstrated a dual signal sensing capability by capitalizing on the intricate interactions occurring at the oil-water-solid multiphase interfaces. Notably, the sensor harnessed two distinct signal sources for its functionality. Firstly, it exploited the electric signals from the contact electrification

This article is protected by copyright. All rights reserved.

Accepted Article

15214095, ja, Downloaded from https://onlinelibrary.wiley.com/doi/10.1002/adma.202308197 by Nanyang Technological University Lee Kong Chian School Of Medicine, Wiley Online Library on [16/10/2023]. See the Terms and Conditions (https://onlinelibrary.wiley.com/terms-and-conditions) on Wiley Online Library for rules of use; OA articles are governed by the applicable Creative Commons License

Accepted Article

and electrostatic induction effect between the liquid medium and the PTFE film. Secondly, the sensor leveraged the electrostatic charges in the electrode induced through the intricate oil/water interfacial charges when the device was inserted into the oil/water interface. This sophisticated integration of multiple signal sources empowered the sensor to exhibit enhanced sensitivity, which could well detect the different dopamine solution with different concentrations. This device also exhibited an excellent ability to sense different chemical solution, as shown in Figure 6a (ii). It has been known that a preferential adsorption of hydroxyl ions (OH^-) would occur at the oil/water interface as the interfacial water molecules would preferentially expose their oxygen atoms towards the hydrophobic phase, creating an environment conducive to the adsorption of OH^- ions.[55] Therefore, an interfacial electrical signal would be detected when the TENG was inserted into the oil/water interface, and this signal was highly affected by the pH values and ion concentration, providing an ideal platform for biochemical sensing.

Corrosion protection is another promising application for liquid-solid TENGs on account of the huge potential of energy harvesting from blue energy. Most metals will deteriorate when they are immersed in marine environments because of the various electrochemical reactions among metals, seawater and dissolved oxygen. In this case, a flexible and area-scalable liquid-solid TENG has been fabricated, which could harvest kinetic wave energy and convert it into electricity for current cathodic protection (Figure 6b).[56] The large-area nanostructured patterns and integration methods enabled a conspicuous enhancement in power output, providing effective corrosion protection toward the cathode. As demonstrated in Figure 6b, the carbon steel was connected to the prepared TENG device and then immersed in a 0.5 mol L^{-1} NaCl solution. The results showed that the surfaces of the carbon steel could be well protected even after 8 hours, while the one without the TENG

This article is protected by copyright. All rights reserved.

15214095, ja, Downloaded from https://onlinelibrary.wiley.com/doi/10.1002/adma.202308197 by Nanyang Technological University Lee Kong Chian School Of Medicine, Wiley Online Library on [16/10/2023]. See the Terms and Conditions (https://onlinelibrary.wiley.com/terms-and-conditions) on Wiley Online Library for rules of use; OA articles are governed by the applicable Creative Commons License

connection showed severe corrosion, indicating the feasibility of this self-powered corrosion protection device for coastal constructions and underwater facilities.

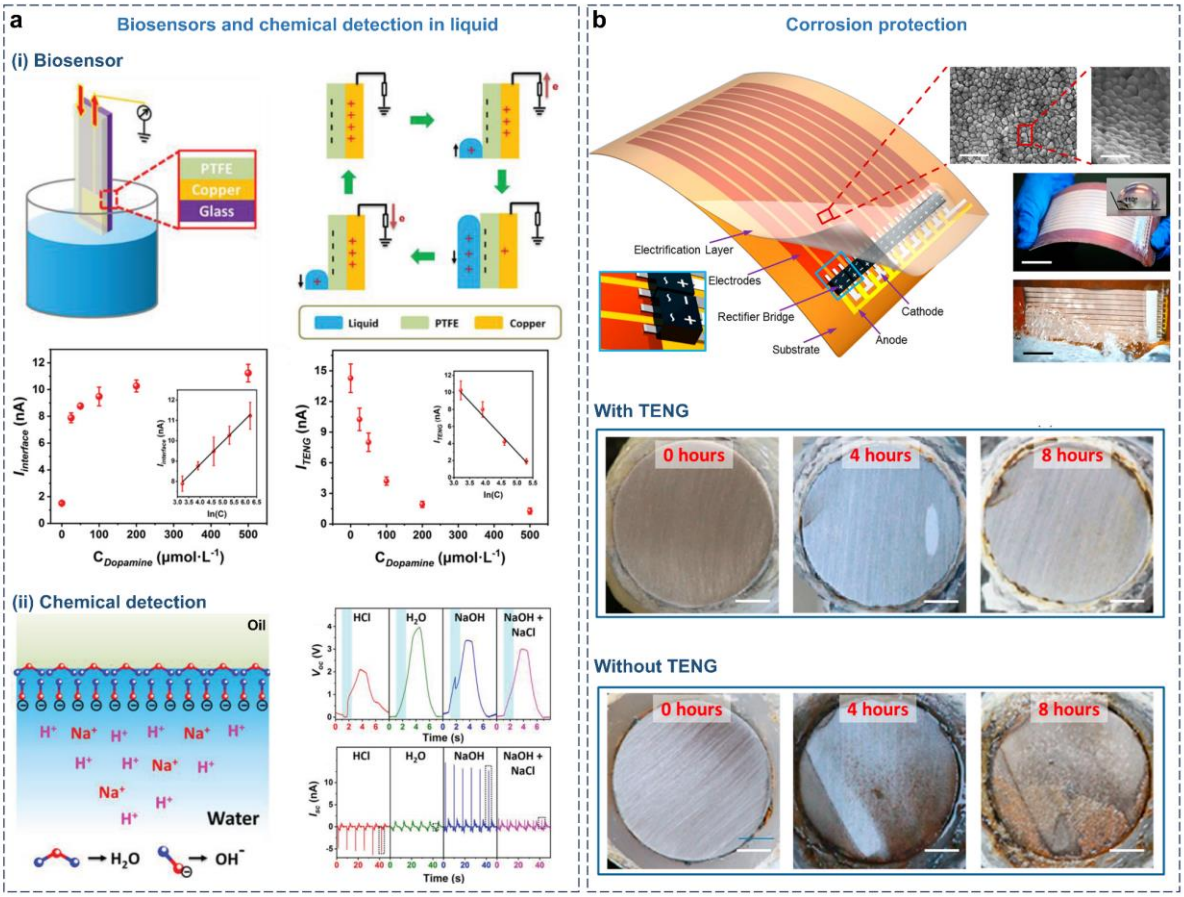

Figure 6. Various applications of liquid-solid TENGs. a) Schematics of self-powered biosensors for detecting dopamine with different concentrations and chemical detection for different chemical solution. Reproduced with permission.[54] Copyright 2019, Wiley-VCH. b) Self-powered cathodic protection system based on liquid-solid TENGs. Reproduced with permission.[56] Copyright 2015, American Chemical Society.

3. Gas-Solid TENG

This article is protected by copyright. All rights reserved.

Accepted Article

15214095, ja, Downloaded from https://onlinelibrary.wiley.com/doi/10.1002/adma.202308197 by Nanyang Technological University Lee Kong Chian School Of Medicine, Wiley Online Library on [16/10/2023]. See the Terms and Conditions (https://onlinelibrary.wiley.com/terms-and-conditions) on Wiley Online Library for rules of use; OA articles are governed by the applicable Creative Commons License

Accepted Article

In contrast to solids and liquids which have fixed or relatively close arrangements of molecules, gases lack strong intermolecular interactions and have no fixed shape or volume. As a result, gas molecules move freely and randomly in all directions, leading to low volume density and presenting challenges in manipulation. In view of these obstacles, the development of gas-solid TENG has long been neglected. Even though some attempts have been made to scavenge wind energy using the triboelectric effect, the device structures have predominantly relied on solid-solid TENGs, while the wind only serves as a driving source to facilitate the contact and separation between two solid surfaces.[57-59] Additional research endeavors have focused on exploring gas-solid two-phase flow sensors that utilize the continuous and high-speed impact of fine particles on a solid substrate.[60-61] However, the high-concentration particle flow and relatively large particle sizes may draw potential safety concerns and impose stringent limitations on their applicability in broader scenarios. In order to address these potential challenges, two innovative strategies have emerged, namely, the design of porous elastomer with discretely closed voids[13] and the development of bubble energy generators[18], opening up new possibilities for the development of stable and high-performance gas-solid TENGs.

3.1. Mechanism

The operational principle of gas-solid TENGs hinges upon the triboelectric effect, which arises from interactions between gases and solid materials. Given that gases lack fixed volumes and exhibit unpredictable movement, it becomes imperative to enclose them within solids or liquids. This enclosure serves a dual purpose: realizing effective gas control and ensuring sufficient friction between the gases and solids. Consequently, two primary operational mechanisms have been

This article is protected by copyright. All rights reserved.

15214095, ja, Downloaded from https://onlinelibrary.wiley.com/doi/10.1002/adma.202308197 by Nanyang Technological University Lee Kong Chian School Of Medicine, Wiley Online Library on [16/10/2023]. See the Terms and Conditions (https://onlinelibrary.wiley.com/terms-and-conditions) on Wiley Online Library for rules of use; OA articles are governed by the applicable Creative Commons License

developed - porous elastomer-based and bubble-based gas-solid TENGs - where gases are either encapsulated within solids or incorporated into liquids, respectively.

3.1.1. Mechanism of Porous Elastomer-Based Gas-Solid TENG

Porous elastomer with controllable and sealed voids provides an ideal platform for gas trapping, rendering an efficient interaction and charge transfer between solid and trapped gas during a periodical compressed process.[13] The working mechanism of this gas-solid TENG is illustrated in **Figure 7**a. When the elastomer undergoes compressive deformation, it generates an immediate pressure surge within its internal voids, resulting in strong contact and friction between trapped gas and elastomer. This intense interaction facilitates the electron transfer from the trapped gas to the elastomer. Once the pressure is released, an instantaneous asymmetric charge distribution will occur within the inner surface of the voids, causing an electric potential difference between the two electrodes via an electrostatic induction effect. Meanwhile, a continuous electric signal will flow through an external circuit until a fully balanced state is achieved. When the elastomer is compressed again, the signal will flow in the opposite direction owing to the reduced electric potential difference induced by the asymmetric distribution of the contrary charges. By repeating this compression-release cycle, continuous and stable alternating current signals can be obtained. The intriguing point for this strategy is the gas can be well captured by the closed voids within the elastomer, so the interaction intensity between solid and gas can be effectively manipulated by the compression force and void size, providing a controllable and stable approach for gas-solid TENG fabrication.

3.1.2. Mechanism of Bubble-Based Gas-Solid TENG

This article is protected by copyright. All rights reserved.

Accepted Article

15214095, ja, Downloaded from https://onlinelibrary.wiley.com/doi/10.1002/adma.202308197 by Nanyang Technological University Lee Kong Chian School Of Medicine, Wiley Online Library on [16/10/2023]. See the Terms and Conditions (https://onlinelibrary.wiley.com/terms-and-conditions) on Wiley Online Library for rules of use; OA articles are governed by the applicable Creative Commons License

Accepted Article

Another promising technique for gas-solid TENG is bubble-based energy generators, as shown in Figure 7b.[18] The device configuration is composed of substrate, electrodes, dielectric material (*e.g.* PTFE), as well as the water layer. In particular, one electrode is placed between the substrate and dielectric material, while the other one is immersed in water. The whole device structure is similar to a field effect transistor containing source, gate and drain terminals. The dielectric material in combination with one electrode serves as the source terminal, and the other electrode immersed in water can be considered as the drain electrode. The moving bubbles that controlled the charge release from the dielectric material surface can be regarded as gate terminals.

The crucial points for fabricating a high-performance bubble energy generator include the selection of dielectric material with high-density surface charges, suitable surface wettability and the two-electrode design. Before the bubble and dielectric material are in contact, a pre-charging procedure should be conducted to maintain a high-density charge distribution at the surface of the dielectric material. When there is no bubble, no electric signals can be detected between the two electrodes due to the screening effect induced by the counterions in water. Once the bubble impinges the surface of the dielectric material, the original liquid/solid interface will be converted into the gas/solid interface promptly. In this case, the electrostatic charge will be induced on the electrode owing to the exposure of the dielectric material surface to the air bubble, resulting in a charge transfer between the two electrodes. On the contrary, limited charges can be transferred for a single electrode design due to the strong screening effect caused by the electrode and the lack of a closed-circuit loop among the electrodes, water and dielectric material. It is worth noting that the electric output performance of this bubble energy generator is independent of the electrode parameters, such as electrode material, size and spatial position, indicating this device can be widely

This article is protected by copyright. All rights reserved.

15214095, ja, Downloaded from https://onlinelibrary.wiley.com/doi/10.1002/adma.202308197 by Nanyang Technological University Lee Kong Chian School Of Medicine, Wiley Online Library on [16/10/2023]. See the Terms and Conditions (https://onlinelibrary.wiley.com/terms-and-conditions) on Wiley Online Library for rules of use; OA articles are governed by the applicable Creative Commons License

applied in various scenarios, especially in underwater energy harvesting and distributed ocean sensors.

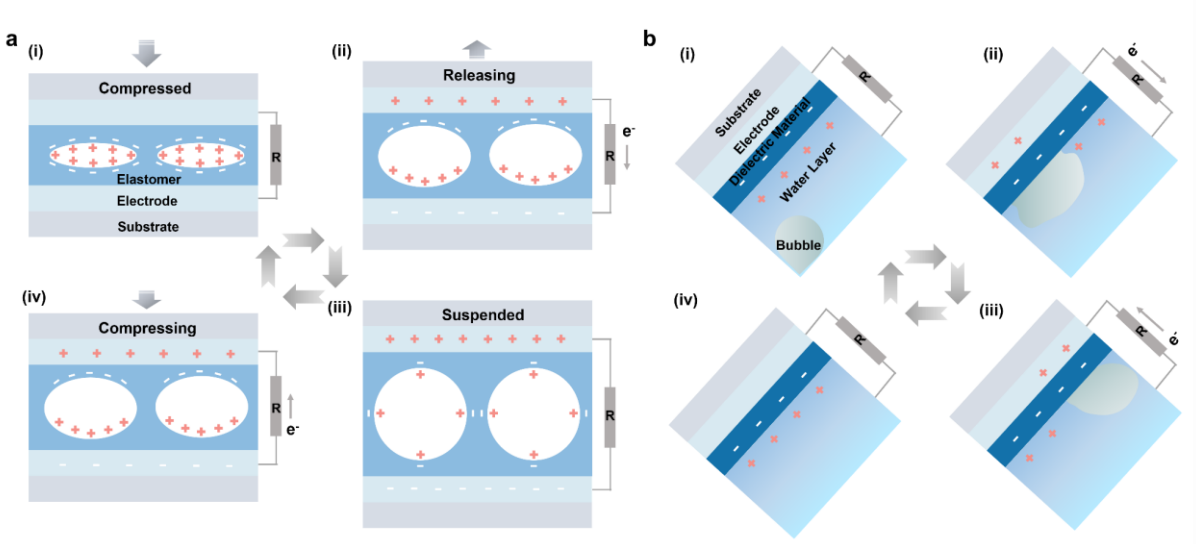

Figure 7. Working mechanism of gas-solid TENGs. a) Working mechanism of porous elastomer-based gas-solid TENG. Reproduced with permission.[13] Copyright 2020, AAAS. b) Working mechanism of bubble-based gas-solid TENG. Reproduced with permission.[18] Copyright 2022, AAAS.

3.2. Optimization Strategies

The optimization of gas-solid TENGs depends on the distinct working principles and structural features of the devices. In the case of porous elastomer-based TENGs, the gases are effectively encapsulated within sealed voids. Consequently, optimization efforts primarily target the design of the porous material itself. This includes considerations such as the synthesis methods for porous elastomers, tuning the material composition, controlling pore structures, and enhancing surface functionalities. Conversely, bubble-based gas-solid TENGs operate in a more dynamic environment, where the release of bubbles and the efficient interaction between bubbles and solid surfaces assume greater significance. In this context, factors like the wettability of the solid surface,

This article is protected by copyright. All rights reserved.

Accepted Article

15214095, ja, Downloaded from https://onlinelibrary.wiley.com/doi/10.1002/adma.202308197 by Nanyang Technological University Lee Kong Chian School Of Medicine, Wiley Online Library on [16/10/2023]. See the Terms and Conditions (https://onlinelibrary.wiley.com/terms-and-conditions) on Wiley Online Library for rules of use; OA articles are governed by the applicable Creative Commons License

synchronized control of multiple bubbles, and rapid bubble collapse become critical elements that can substantially influence the contact-separation efficiency and the charge transfer process for power generation. This section will delve into more comprehensive optimization strategies for both types of gas-solid TENGs, considering their distinctive characteristics and operational intricacies.

3.2.1. Performance Optimization of Porous Elastomer-Based Gas-Solid TENG

Material design is the priority for the fabrication of high-performance porous elastomer-based gas-solid TENG. The selected material should possess a superior elasticity, in other words, excellent shape recovery even after being stretched or compressed, enabling the material to endure long-term and stable compression-release cycles. In this instance, various methodologies, including block copolymer self-assembly[62-63], template-assisted synthesis[64-65], as well as aerogels preparation[66-67], could be utilized to design porous elastomers with excellent mechanical flexibility and functional customizability (**Figure 8**a). Composition optimization is another strategy that can enhance electric performance and simultaneously bestow multifunctionality on the porous elastomer. For instance, by combining various functional fillers (*e.g.* graphene oxide nanosheets (GO NSs), $BaTiO_3$ nanoparticles (BTO NPs) and carboxylated multiwalled carbon nanotubes (CMWCNTs)) with the waterborne polyurethane and hydroxyethyl cellulose, a hybrid aerogel with a three-dimensional (3D) honeycomb-like network structure has been prepared (Figure 8b).[66, 68] Particularly, waterborne polyurethane provides the main elastomer framework that crosslinked with GO NSs, BTO NPs and CMWCNTs to form a hybrid aerogel, while hydroxyethyl cellulose serves as both dispersive and adhesive agents that foster the gelation as well as the formation of hydrogen bonding between the polymer backbone and different functional fillers, establishing a stable 3D porous conductive framework with excellent elasticity and mechanical strength. By virtue of this configuration, a gas-

This article is protected by copyright. All rights reserved.

Accepted Article

15214095, ja, Downloaded from https://onlinelibrary.wiley.com/doi/10.1002/adma.202308197 by Nanyang Technological University Lee Kong Chian School Of Medicine, Wiley Online Library on [16/10/2023]. See the Terms and Conditions (https://onlinelibrary.wiley.com/terms-and-conditions) on Wiley Online Library for rules of use; OA articles are governed by the applicable Creative Commons License

Accepted Article

solid/solid-solid coupled TENG has been designed with prominent performance enhancement, whereas the hybrid aerogel can function as both a current collector and charge contributor to improve the electric output.

Intrinsically high negative triboelectricity and long charge retention capacity are also key properties for performance improvement, which allow the strong interaction and efficient charge transfer between the gas and solid. For example, a self-healing and adhesive polysiloxane-dimethylglyoxime–based polyurethane (PDPU) with extremely high negative surface potential has been prepared.[13] In this design, the remarkable dynamic nature of isophorone diisocyanate (IPDI)-derived urethane (-NH-CO-O) promoted the formation of multiple functional units with strong electron affinity (*e.g.* oxime-urethane unit), contributing to the charge trapping and accumulation process of the elastomer. In the meanwhile, various types of supramolecular interactions were widely distributed in the polymer network, endowing the whole elastomer with exceptional adhesion and self-healing ability, which can be utilized in conformable sensors for smart haptics and health monitoring.

The structural characteristics of porous elastomers are also critical to enhance the electric performance of the energy harvester. Some important parameters, such as the pore geometry and size, pore density and surface area, as well as pore surface functionality, will substantially affect the charge transfer efficiency at the gas-solid interface (Figure 8c). Suitable pore geometry and size play vital roles in the electric performance modulation of gas-solid TENG. Different pore geometries, such as spherical, square and tubular networks, will trigger different mechanical deformation rates in conjunction with varying strain distribution along the internal pore edge, resulting in different interfacial interactions between the gas and elastomer. Pore size and density also have a similar

This article is protected by copyright. All rights reserved.

15214095, ja, Downloaded from https://onlinelibrary.wiley.com/doi/10.1002/adma.202308197 by Nanyang Technological University Lee Kong Chian School Of Medicine, Wiley Online Library on [16/10/2023]. See the Terms and Conditions (https://onlinelibrary.wiley.com/terms-and-conditions) on Wiley Online Library for rules of use; OA articles are governed by the applicable Creative Commons License

Accepted Article

influence on the gas/solid interaction but there is a performance balance between these two parameters. On one hand, elastomers with small voids can hold a high-density pore distribution, facilitating a higher pore surface area and more interactions at the gas/solid interface. Nonetheless, when the pores are too small, the closed pores are also hard to be effectively compressed owing to the limited mechanical deformation. On the other hand, large voids will reduce the pore density of the elastomer but promote a more sufficient interfacial interaction and charge transfer process under a strong compressed state. Hence, optimum performance can be realized by modulating both pore size and density.

Apart from pore structure control, surface functionalities are also crucial factors for performance advancement. Pre-modification of monomers and post-treatment of the porous framework are two main approaches that can modulate the functional groups and physicochemical properties of both porous surface and elastomer skeleton.[69] These approaches can regulate the gas affinity and permeance of the material, thus affecting the gas absorption and separation as well as charge trapping and storing capacity. If the porous elastomers have strong gas absorption ability, a relatively stable gas layer may concentrate on the internal surface of the pores, which may weaken the interaction between the gas and solid during the compressing process, on account of the decreased number of impacting gas molecules that freely distributed in the void.[65] Furthermore, a high negative surface potential can be achieved by introducing various strong electron-withdrawing groups, such as -F, -CF_3, and -CF=CF_2, to the main chain of the elastomer, boosting the electric output performance.[70]

This article is protected by copyright. All rights reserved.

15214095, ja, Downloaded from https://onlinelibrary.wiley.com/doi/10.1002/adma.202308197 by Nanyang Technological University Lee Kong Chian School Of Medicine, Wiley Online Library on [16/10/2023]. See the Terms and Conditions (https://onlinelibrary.wiley.com/terms-and-conditions) on Wiley Online Library for rules of use; OA articles are governed by the applicable Creative Commons License

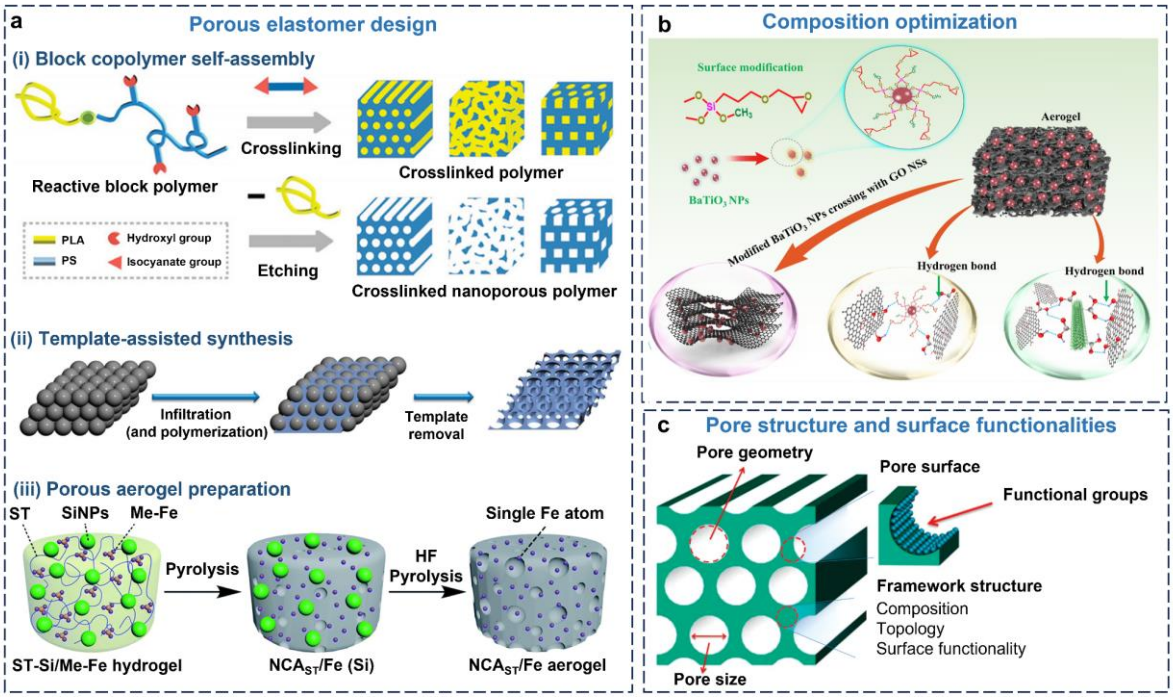

Figure 8. Performance optimization of porous elastomer-based gas-solid TENG. a) Various design strategies for porous elastomers with excellent mechanical flexibility and functional customizability: (i) Block copolymer self-assembly method. Reproduced with permission.[63] Copyright 2011, American Chemical Society. (ii) Template-assisted synthesis. Reproduced with permission.[65] Copyright 2012, American Chemical Society. (iii) Porous aerogel preparation. Reproduced with permission.[67] Copyright 2019, Royal Society of Chemistry. b) Composition optimization for high-performance and multifunctional porous elastomer-based gas-solid TENG design. Reproduced with permission.[68] Copyright 2023, American Chemical Society. c) Pore structure design and surface functionality optimization for high-performance porous elastomer preparation. Reproduced with permission.[65] Copyright 2012, American Chemical Society.

3.2.2. Performance Optimization of Bubble-Based Gas-Solid TENG

The material requirement for high-performance bubble-based gas-solid TENG is analogous to the porous elastomer, which also needs high-density surface charges and long charge retention capacity,

This article is protected by copyright. All rights reserved.

Accepted Article

15214095, ja, Downloaded from https://onlinelibrary.wiley.com/doi/10.1002/adma.202308197 by Nanyang Technological University Lee Kong Chian School Of Medicine, Wiley Online Library on [16/10/2023]. See the Terms and Conditions (https://onlinelibrary.wiley.com/terms-and-conditions) on Wiley Online Library for rules of use; OA articles are governed by the applicable Creative Commons License

Accepted Article

but the bubble energy generator raises higher demands for surface wettability modulation on account of the gas removal efficiency. To reveal the relationship between the dielectric surface wettability and the electric output, Yan et al. delved into the influence of bubble contact angles on the transferred charge density and bubble mobility of the energy generator.[18] Specifically, the transferred charge density would increase at first and then decrease when the bubble contact angle increases from ~45° to ~115°, as a result of the balance of the bubble contact area and the water layer coverage. For example, the water layer can be efficiently drained by the continuous bubble impact when the bubble contact angle is 65°, thereby eradicating the undesired screening effect (**Figure 9**a). On the contrary, a continuous water film will cover the surface of dielectric material when the bubble contact angle equals 135°, which impedes the contact between bubbles and dielectric material and further suppresses the charge release from the dielectric materials.

On the other hand, the bubble mobility, quantified by the interfacial energy required to overcome the van der Waals force, would linearly diminish with the increment of bubble contact angle, which has been confirmed by the corresponding molecular dynamics analysis (Figure 9b). Accordingly, an optimum wettability with the highest electric performance can be obtained by combining both transferred charge density and bubble mobility. More quantitatively, a theoretical model that reflects the relationship between the output voltage and various impact factors (*e.g.* bubble contact angle, surface tension and water viscosity) has been proposed (Figure 9c), matching well with the experimental results (Figure 9d and 9e), which further confirmed the crucial roles of surface wettability on the electric performance of the bubble-based gas-solid TENG.

This article is protected by copyright. All rights reserved.

15214095, ja, Downloaded from https://onlinelibrary.wiley.com/doi/10.1002/adma.202308197 by Nanyang Technological University Lee Kong Chian School Of Medicine, Wiley Online Library on [16/10/2023]. See the Terms and Conditions (https://onlinelibrary.wiley.com/terms-and-conditions) on Wiley Online Library for rules of use; OA articles are governed by the applicable Creative Commons License

Accepted Article

Multiple bubble synchronization and fast bubble collapse are also important optimization strategies for enhancing the output performance of bubble energy generators. Preliminary results have shown that synchronic bubbles would display a higher electric output owing to the synergistic collision from different bubbles, while in a non-synchronization mode, bubbles would be released at different intervals, resulting in an asynchronous spreading and recoiling processes among different bubbles (Figure 9f).[18] Hence, some electric signals from various bubbles may cancel each other and thus cause reduced and erratic electric outputs. Rapid bubble collapse is also imperative for efficient energy generation, which can facilitate the fast and continuous electrostatic induction and charge transfer process. By transforming the aquatic environment into an air environment, the bubble collapse time can be reduced to around 25% of the original (Figure 9g). At the same time, the undesired screening effect induced by the water layer could also be excluded. Furthermore, compared to droplet-based energy generators, bubble-based gas-solid TENG shows a longer electricity generation duration and charge retention capacity owing to the small spreading area. In view of these advantages, the electric output of the energy generator can be significantly enhanced.

This article is protected by copyright. All rights reserved.

15214095, ja, Downloaded from https://onlinelibrary.wiley.com/doi/10.1002/adma.202308197 by Nanyang Technological University Lee Kong Chian School Of Medicine, Wiley Online Library on [16/10/2023]. See the Terms and Conditions (https://onlinelibrary.wiley.com/terms-and-conditions) on Wiley Online Library for rules of use; OA articles are governed by the applicable Creative Commons License

Accepted Article

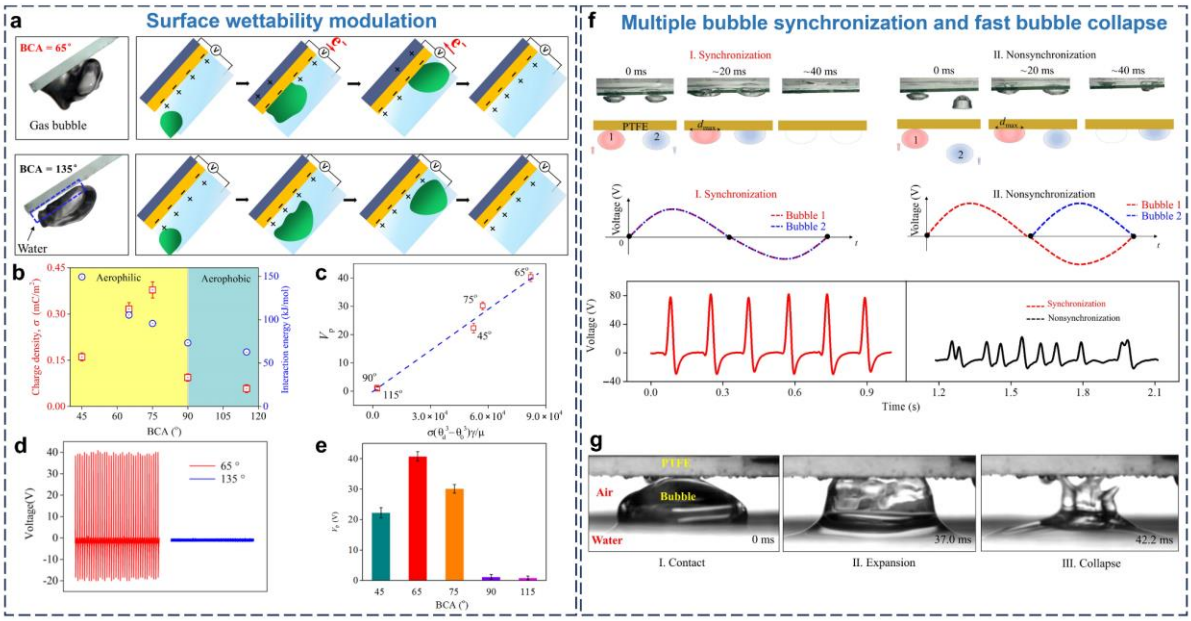

Figure 9. Performance optimization of bubble-based gas-solid TENG. a) Different interactions between the bubble and the dielectric surface with a bubble contact angle of 65° and 135°. b) Charge density and calculated gas-solid interaction energy under varying bubble contact angles. c) Linear relationship between output voltage (V_p) and σ ($\vartheta_d^3 - \vartheta_0^3$) γ/μ, where σ is the charge density; ϑ_d is the dynamic contact angle; ϑ_0 is initial bubble contact angle; γ is the surface tension and μ is the water viscosity. d) Output voltage of bubble-based gas-solid TENG with bubble contact angles of 65° and 135°. e) Output voltage of bubble-based gas-solid TENG with varying bubble contact angles from 45° to 115°. f) Photograph, schematic as well as the corresponding electric output analysis and experimental results of bubble collision process under synchronic mode (I) and nonsynchronic mode (II). g) The bubble contact, expansion, and collapse process in the air. Reproduced with permission.[18] Copyright 2022, AAAS.

3.3. Advantages and Possible Applications of Gas-Solid TENG

Traditional solid and liquid-based TENGs usually require the full contact and separation of two different phases to realize the charge transfer via external circuits, but this process may restrain

This article is protected by copyright. All rights reserved.

15214095, ja, Downloaded from https://onlinelibrary.wiley.com/doi/10.1002/adma.202308197 by Nanyang Technological University Lee Kong Chian School Of Medicine, Wiley Online Library on [16/10/2023]. See the Terms and Conditions (https://onlinelibrary.wiley.com/terms-and-conditions) on Wiley Online Library for rules of use; OA articles are governed by the applicable Creative Commons License

most application scenarios. In addition, their electric outputs are also restricted by the ambient environment and effective contact areas, setting limitations on the stability and accuracy of triboelectricity-driven sensors. In light of these challenges, porous elastomer-based TENGs provide a more stable and simple operation mode where the gas can be well encapsulated within the closed voids, indicating no additional phase is needed to trigger the contact-separation process. In the meanwhile, the interaction between the gas and solid can be effectively controlled via the applied pressure and pore structure design, and the output performance is less affected by external contamination and ambient humidity considering the sealed and stable environment within the pores, offering new ideas for high-precision sensor fabrication. Based on these advantages, some trials have been conducted to construct self-powered electronic skin for the detection of various physiological and human motion signals. For example, Xiong et al. developed a sticky PDPU-based gas-solid TENG with excellent deformation resistance (*e.g.* twisting, bending and stretching) and pressure sensitivity (0.017 V kPa^{-1}), which can be attached to different parts of the human body for multimodal gesture monitoring, such as gait recognition and finger bending (**Figure 10**a).[13] Huang et al. also designed a series of hybrid aerogel-based gas-solid/solid-solid TENGs that are not only used for energy harvesters but also serve as self-powered sensors for handwriting detection and palm strokes.[66, 68]

Different from the porous elastomer-based gas-solid TENGs, bubble-based energy generators are more suitable for dynamic and complex underwater environments. A giant number of bubbles would be constantly created from the river, lakes and ocean, as a result of the gas release from temperature and salinity differences, chemical pollutants reacting with water, as well as the various biological activities such as respiration and metabolism. Under these circumstances, energy

This article is protected by copyright. All rights reserved.

Accepted Article

15214095, ja, Downloaded from https://onlinelibrary.wiley.com/doi/10.1002/adma.202308197 by Nanyang Technological University Lee Kong Chian School Of Medicine, Wiley Online Library on [16/10/2023]. See the Terms and Conditions (https://onlinelibrary.wiley.com/terms-and-conditions) on Wiley Online Library for rules of use; OA articles are governed by the applicable Creative Commons License

Accepted Article

harvesting from small bubbles is critical to accommodate continuous energy outputs and long-term operation stability in a marine environment. By means of pre-charged PTFE and two-electrode design, Yan et al. prepared a transistor-inspired bubble energy generator with a record-high power density among all existing bubble-based TENGs.[18] The maximum power density of this device could achieve 56.4 W m^{-3}, which could drive LEDs, multifunctional sensors and wireless transmitters. Other attractive applications, such as tube leakage detection[71], water level monitoring[72] and gas flow sensors[73], have been explored as well (Figure 10b-d), suggesting the great potential of bubble-based TENGs in underwater energy harvesting and self-powered sensors.

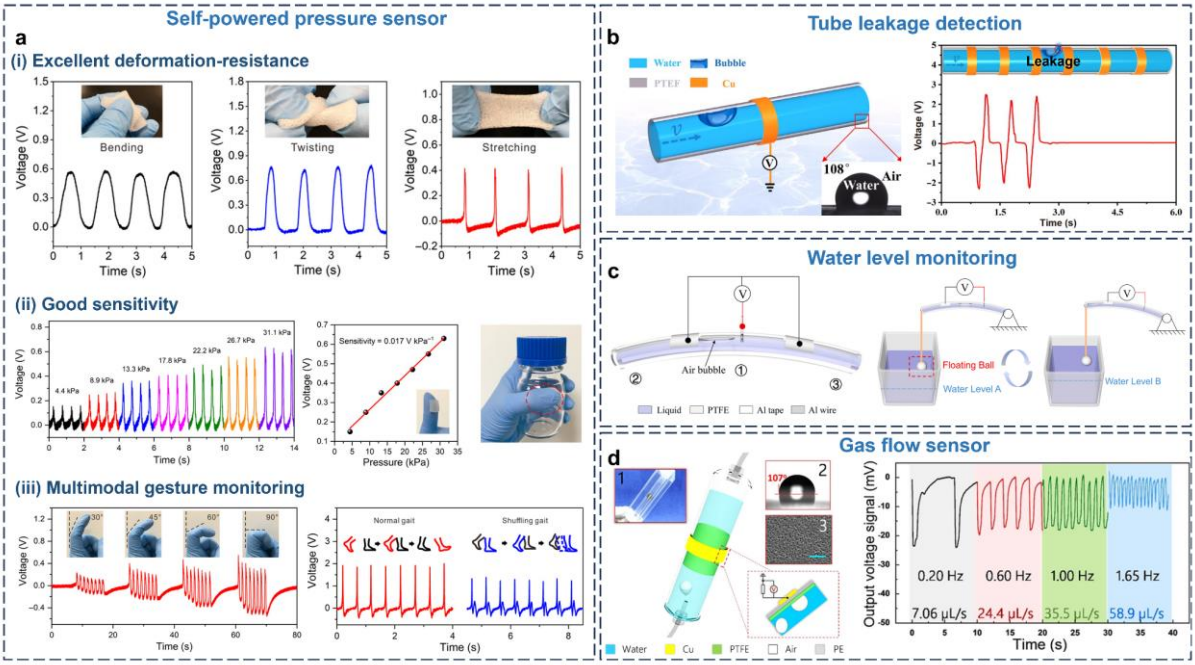

Figure 10. Diverse applications of gas-solid TENGs. a) Porous PDPU-based gas-solid TENGs with excellent deformation resistance and pressure sensitivity exhibiting their great potential in multimodal gesture monitoring such as finger bending and gait recognition. Reproduced with permission.[13] Copyright 2020, AAAS. Bubble-based energy generators displaying their abundant applications: b) Tube leakage detection. Reproduced with permission.[71] Copyright 2021, Springer

This article is protected by copyright. All rights reserved.

15214095, ja, Downloaded from https://onlinelibrary.wiley.com/doi/10.1002/adma.202308197 by Nanyang Technological University Lee Kong Chian School Of Medicine, Wiley Online Library on [16/10/2023]. See the Terms and Conditions (https://onlinelibrary.wiley.com/terms-and-conditions) on Wiley Online Library for rules of use; OA articles are governed by the applicable Creative Commons License

Nature. c) Water level monitoring. Reproduced with permission.[72] Copyright 2022, Elsevier. d) Gas flow sensor. Reproduced with permission.[73] Copyright 2016, American Chemical Society.

4. Liquid-Liquid and Gas-Liquid TENG

As extensions to the fluid-solid TENGs, the exploration of the liquid-liquid and gas-liquid energy generators has also been initiated, driven by their immense potential to overcome specific limitations of solid-based TENGs, such as surface contamination, interfacial defects and restricted contact separation frequency. Various liquid-liquid TENGs have already been proposed, encompassing water-oil immiscible systems, liquid membrane-based designs and magnetically controlled configurations.[74-75] Although investigations on gas-liquid TENGs are still in the preliminary stage, it is worth noting that power generation from gas-liquid interactions is not a novel phenomenon, as observed in natural occurrences like lightning on rainy days[76]. This observation underscores the tremendous potential for gas-liquid TENGs, which could offer ultrahigh electric outputs in the future. Despite some remarkable advancements, the limited mechanistic understanding of charge transfer and dissipation processes at the fluid interface hinders the full utilization of these new types of electric generators. Therefore, this section will provide a comprehensive overview of the current research progress and present a systematic mechanism summary for both liquid-liquid and gas-liquid TENGs.

4.1. Mechanism

The operational mechanism of all-fluid-based TENGs also relies on contact electrification and interfacial charge transfer between distinct fluid mediums. In the context of all-liquid-based TENGs, it is paramount to establish an immiscible liquid interface while achieving precise flow control for the

This article is protected by copyright. All rights reserved.

Accepted Article

15214095, ja, Downloaded from https://onlinelibrary.wiley.com/doi/10.1002/adma.202308197 by Nanyang Technological University Lee Kong Chian School Of Medicine, Wiley Online Library on [16/10/2023]. See the Terms and Conditions (https://onlinelibrary.wiley.com/terms-and-conditions) on Wiley Online Library for rules of use; OA articles are governed by the applicable Creative Commons License

Accepted Article

device fabrication. In this regard, liquid droplets serve as effective manipulation tools, enabling systematic exploration of the charge transfer processes within various liquid environments. For instance, droplets can be precisely directed to descend within different types of liquid mediums or pass through liquid membranes. They can also make direct contact with other immiscible liquid droplets, furnishing a quantitative means to assess charge transfer behaviors among diverse liquids. When the fluid interfaces involve gases, the manipulation of gas presents a more intricate challenge. Consequently, an alternative approach for studying gas-liquid charge transfer is to control the liquid phase. One promising technique is the acoustic levitation method, which facilitates the suspension and rotation of droplets within a gas-filled environment. This technique provides an ideal platform for gaining insights into the phenomena of contact electrification and charge transfer processes occurring at the gas-liquid interface.

An illustrative example of a liquid-liquid TENG featuring droplets descending within an immiscible liquid environment is depicted in **Figure 11**a.[77] When the water droplet falls into the oil, the tribo-motion at the water-oil interface will promote the surface charge accumulation of the droplet. Once the water droplet passes through the single-electrode frame placed at the bottom of the oil, the accumulated charges will be transferred to the electrode via an electrostatic induction effect (Figure 11a (ii)). With the continuous falling of water droplets, the contact interface can be dynamically refreshed, so a periodical displacement current can be generated through the external circuit. This fundamental liquid-liquid TENG structure can be extended to other systems, such as liquid droplet-membrane systems, establishing a design guidance for continuous liquid energy harvesting.[10, 78] Recently, a more precise manipulation approach of liquid droplets has been developed based on immiscible interface construction, as shown in Figure 11b.[16] Similar to solid-based TENGs, when two

This article is protected by copyright. All rights reserved.

15214095, ja, Downloaded from https://onlinelibrary.wiley.com/doi/10.1002/adma.202308197 by Nanyang Technological University Lee Kong Chian School Of Medicine, Wiley Online Library on [16/10/2023]. See the Terms and Conditions (https://onlinelibrary.wiley.com/terms-and-conditions) on Wiley Online Library for rules of use; OA articles are governed by the applicable Creative Commons License

different liquid droplets come into contact, charges will be transferred from one droplet to the other at the interface. During the separation process, the charge imbalance induces a potential difference between the electrodes, and electrons will flow through the external circuit and generate instantaneous current signals. Compared with the previous structure, this immiscible droplet-based TENG provides a more quantitative and stable approach to investigate charge transfer behaviors at liquid interface.

Through the simulation of electrostatic charge accumulation in suspended liquid droplets within clouds, an acoustic levitation method focusing on gas-liquid interaction has been proposed. This innovative approach involves precise control of liquid droplet suspension through the harmonious interplay of acoustic and electric fields, as depicted in Figure 11c.[76] Within the acoustic field, the suspended droplets undergo rapid rotation, inducing robust friction between the liquid and the ambient gas medium. This dynamic process triggers contact electrification at the gas-liquid interface, leading to the accumulation of electric charges within the droplets. The charge accumulation in the droplets is further governed by the balance between the electric field force applied to the droplets and the acoustic trap force. Consequently, the charge quantity of the droplets can be accurately determined through the calculation of force equilibrium. This acoustic levitation method not only presents a non-contact charge measurement tool of high precision but also furnishes a stable and controllable platform for investigating the intricate charge transfer mechanisms between various liquids and gases.

This article is protected by copyright. All rights reserved.

Accepted Article

15214095, ja, Downloaded from https://onlinelibrary.wiley.com/doi/10.1002/adma.202308197 by Nanyang Technological University Lee Kong Chian School Of Medicine, Wiley Online Library on [16/10/2023]. See the Terms and Conditions (https://onlinelibrary.wiley.com/terms-and-conditions) on Wiley Online Library for rules of use; OA articles are governed by the applicable Creative Commons License

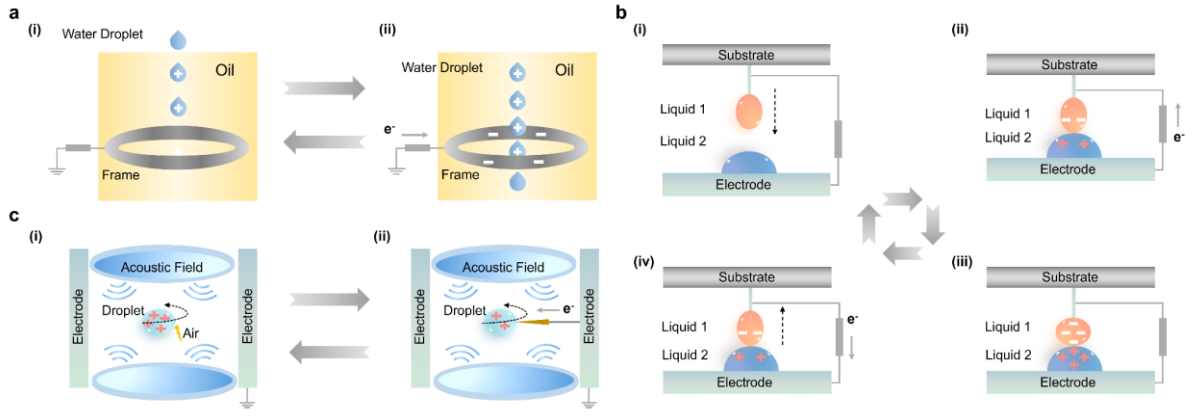

Figure 11. The working mechanism of liquid-liquid and gas-liquid TENGs. a) Working mechanism of liquid-liquid TENG with single-electrode working mode. Reproduced with permission.[77] Copyright 2021, Elsevier. b) Working mechanism of liquid-liquid TENG with contact-separation working mode. Reproduced with permission.[16] Copyright 2022, Springer Nature. c) Working mechanism of levitated drop-based gas-liquid TENG. Reproduced with permission.[76] Copyright 2021, American Chemical Society.

4.2. Optimization Strategies

The existing optimization strategies for all-fluid-based TENGs primarily focus on two aspects: composition modulation and interface engineering. Composition modulation involves the regulation of liquid or gas components, ion concentrations, and pH levels. This approach offers a direct and highly effective means to tailor the physicochemical properties of the fluids involved, thereby exerting a significant influence on the charge transfer dynamics and electric output of FB-TENGs. Another avenue for optimization is the engineering of interfacial characteristics between the fluids. Various strategies, such as the creation of immiscible liquid-liquid interfaces and the enhancement of gas flow speed or vibration frequency, prove to be efficient methods for optimizing interfacial conditions. These optimizations are aimed at improving contact electrification and charge transfer

This article is protected by copyright. All rights reserved.

Accepted Article

15214095, ja, Downloaded from https://onlinelibrary.wiley.com/doi/10.1002/adma.202308197 by Nanyang Technological University Lee Kong Chian School Of Medicine, Wiley Online Library on [16/10/2023]. See the Terms and Conditions (https://onlinelibrary.wiley.com/terms-and-conditions) on Wiley Online Library for rules of use; OA articles are governed by the applicable Creative Commons License

efficiency. In this section, the above optimization strategies will be discussed in detail, providing a comprehensive understanding of the factors influencing power generation in all-fluid-based TENGs.

To explore the influence of liquid composition on the electric performance of all-liquid-based TENGs, a series of experiments have been conducted to reveal the contact electrification in diverse liquid-liquid systems, such as oleic acid (OA)-water interface, hexadecane (Hex)-water interface and hydrofluoroether (HFE)-water interface (**Figure 12**a).[78] From the results, Hex-water system exhibited a propensity for preferential adsorption of ions, alongside the coexistence of electron transfer phenomena at the interface. In contrast, the OA-water system was primarily governed by the dissociation of functional groups, accompanied by concurrent ion adsorption. This behavior rendered the OA-water system highly susceptible to H^+, as H^+ significantly influenced both the group dissociation process and the preferential adsorption of OH^-. In the HFE-water system, electron transfer played a dominant role at the interface. Consequently, this system exhibited the least susceptibility to H^+, since the influence of H^+ was predominantly confined to the preferential adsorption of OH^-, with a lesser effect on electron transfer. After the elucidation of various mechanisms, HFE was considered a promising liquid material for energy harvesting from weak acid rainwater environments, attributed to its resilience to the influence of H^+. Moreover, OA exhibits its advantages in seawater energy harvesting because the functional group dissociation would be least affected by high salt concentrations.

Another strategy for optimizing liquid-liquid TENGs is to generate a reliable and immiscible liquid-liquid interface to solve the issues of high interfacial viscosity and surface tension for various liquids, which can overcome the low output efficiency caused by the difficult contact-separation process. To tackle this challenge, dextran (DEX) and polyethylene glycol (PEG) were utilized to construct a

This article is protected by copyright. All rights reserved.

Accepted Article

15214095, ja, Downloaded from https://onlinelibrary.wiley.com/doi/10.1002/adma.202308197 by Nanyang Technological University Lee Kong Chian School Of Medicine, Wiley Online Library on [16/10/2023]. See the Terms and Conditions (https://onlinelibrary.wiley.com/terms-and-conditions) on Wiley Online Library for rules of use; OA articles are governed by the applicable Creative Commons License

recoverable and immiscible aqueous-aqueous interface (Figure 12b), which allowed different solutes to induce phase separation and redistribution in the water.[16] This aqueous two-phase TENG could well maintain the droplet shape by virtue of the surface tension control, achieving a 129 nC charge transfer for a single droplet, which laid the basis for the future development of aqueous electronics and implantable electronic devices.

Apart from the liquid composition optimization and immiscible interface design, enhancing fluid flow is also a favorable approach to enhance the electric performance of FB-TENGs. As illustrated in Figure 12c, a notable increase in electrical potential difference has been successfully attained through the precise control of saltwater flow across microchannels. These microchannels were pre-saturated with low-dielectric constant fluids (*e.g.* oil), so their surfaces were heterogeneous.[79] This special design created alternating zones of slip and non-slip characteristics for the saltwater flow, which induced an uneven shear plane within the system, potentially leading to local concentration polarization and enhancement of electric field propagation efficiency from the channel wall. After the optimization of the dielectric fluids and nanochannel structure, a high electric potential difference with a figure of merit factor of 1.4 has been obtained, establishing the foundation for surface charge engineering and electrokinetic control for FB-TENGs.

The investigations for high-performance gas-liquid TENG design are still in the initial phase considering the intractable challenges of low density of gas and the complex control at the two-phase interface. In this situation, the acoustic levitation technique provides an ideal platform to quantitively investigate the charge transfer between the liquid droplet and various gases. As shown in Figure 12d, the gases were filled within the closed acoustic levitation chamber to ensure complete contact between gas and droplet.[76] In this particular scenario, it was observed that both the

This article is protected by copyright. All rights reserved.

Accepted Article

15214095, ja, Downloaded from https://onlinelibrary.wiley.com/doi/10.1002/adma.202308197 by Nanyang Technological University Lee Kong Chian School Of Medicine, Wiley Online Library on [16/10/2023]. See the Terms and Conditions (https://onlinelibrary.wiley.com/terms-and-conditions) on Wiley Online Library for rules of use; OA articles are governed by the applicable Creative Commons License

transferred charge and the induced current exhibited an increase as the levitation time extended. The process of continuous suspension, coupled with the high-speed rotation of the droplet and strong friction between the droplet and surrounding gases, resulted in a consistent charge accumulation until a saturation state. This phenomenon served as strong evidence for the occurrence of charge transfer between the gas and the liquid phases.

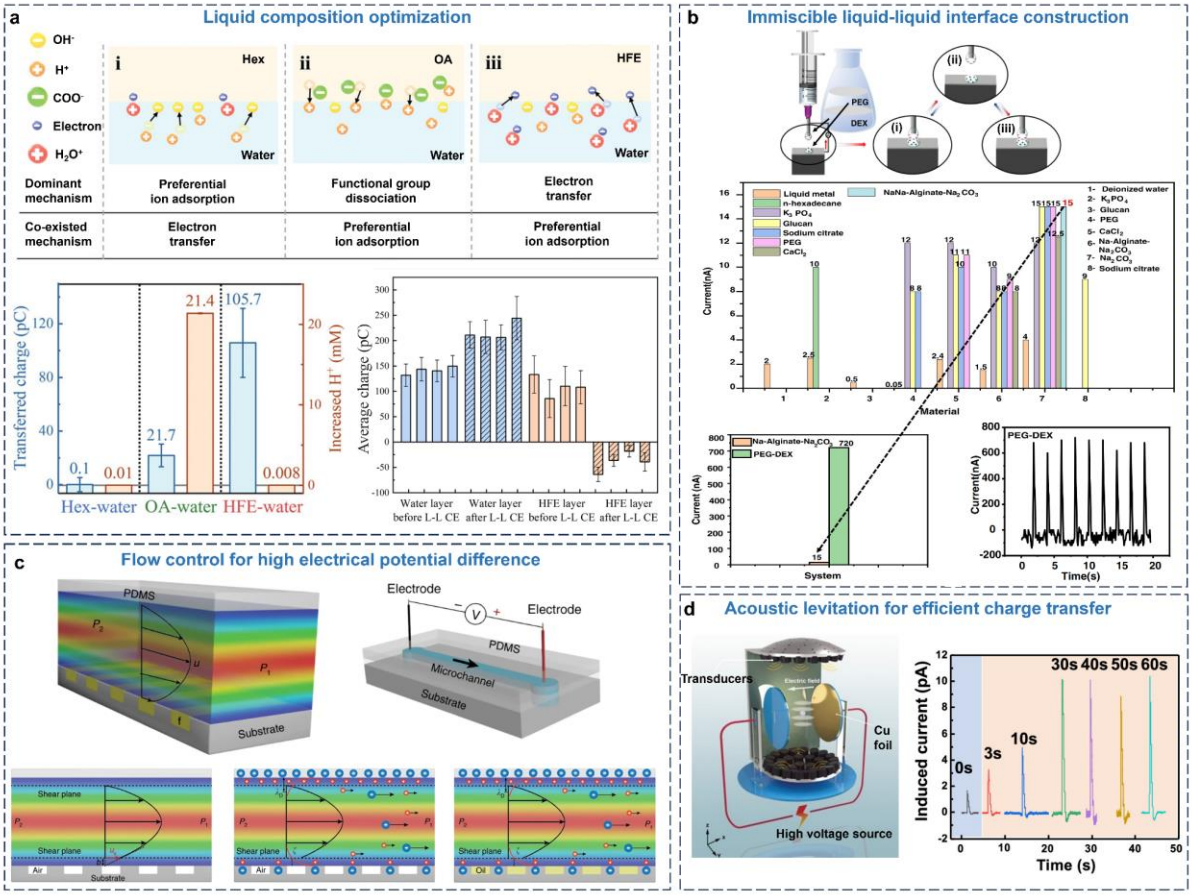

Figure 12. Optimization strategies for all-fluid-based TENGs. a) Working mechanisms for different liquid-liquid TENGs under various liquid compositions as well as the corresponding electric performance optimization for different liquid-liquid interfaces. Reproduced with permission.[78] Copyright 2022, Wiley-VCH. b) Demonstration of the immiscible aqueous-aqueous interface as well as the electric performance optimization of different aqueous two-phase systems. Reproduced with

This article is protected by copyright. All rights reserved.

Accepted Article

15214095, ja, Downloaded from https://onlinelibrary.wiley.com/doi/10.1002/adma.202308197 by Nanyang Technological University Lee Kong Chian School Of Medicine, Wiley Online Library on [16/10/2023]. See the Terms and Conditions (https://onlinelibrary.wiley.com/terms-and-conditions) on Wiley Online Library for rules of use; OA articles are governed by the applicable Creative Commons License

permission.[16] Copyright 2022, Springer Nature. c) Working mechanism of fluid flow over a fluid-filled microchannel for the generation of streaming potential. Reproduced with permission.[79] Copyright 2018, Springer Nature. d) Schematic of acoustic levitation technique for droplets and the enhanced output of induced current with the increase of levitation time. Reproduced with permission.[76] Copyright 2021, American Chemical Society.

4.3. Advantages and Possible Applications of Liquid-Liquid and Liquid-Solid TENGs

All-fluid-based TENGs hold the potential to surmount the inherent limitations of fluid-solid TENGs, such as restricted contact-separation frequencies and the complex control of solid surface wettability, which realize better phase separation efficiency and ample interfacial contact time, consequently facilitating the design of high-performance FB-TENGs. Notably, a novel gas-liquid TENG configuration with continuous and stable power output has been successfully realized by employing a Venturi-like design and capitalizing on the rheological characteristics of gas-liquid two-phase flow (**Figure 13**a).[17] In this innovative design, a high-speed airflow was directed towards the inner side of the PTFE tube, engendering a negative pressure at the top of the vertical capillary. As a result of this pressure difference induced by the Venturi effect, the bottom liquids were propelled upward, transforming into ionized molecules under the forceful impact of the airflow. Then the gas-liquid two-phase flow would be positively charged through the frictional electrification with the PTFE tube. Ultimately, the accumulated negative charges within the tube were discharged to the electrode, generating the output current. The promising aspect of this device structure was derived from the utilization of a gas-liquid two-phase flow based on the Venturi effect. Compared to pure air, gas-liquid flow was more susceptible to breakdown discharge, as water molecules also contributed a greater number of negative ions during the discharging process. Through this improved phase

This article is protected by copyright. All rights reserved.

Accepted Article

15214095, ja, Downloaded from https://onlinelibrary.wiley.com/doi/10.1002/adma.202308197 by Nanyang Technological University Lee Kong Chian School Of Medicine, Wiley Online Library on [16/10/2023]. See the Terms and Conditions (https://onlinelibrary.wiley.com/terms-and-conditions) on Wiley Online Library for rules of use; OA articles are governed by the applicable Creative Commons License

separation efficiency and interfacial contact area, an ultra-high power output (3789 V, 143.6 kW m^{-3}) was achieved, which could directly drive a 24-watt commercial lamp and 1500 LEDs.

In addition to delivering high output performance, fluid-fluid TENGs also offer compelling solutions to the challenges encountered in conventional solid-based TENGs, particularly concerning interfacial contamination and limited effective contact area. As demonstrated in Figure 13b, a lubricant-impregnated porous surface was employed to fabricate liquid-liquid TENGs.[80] This specialized lubricant layer, characterized by its slippery nature and flexibility, not only mitigated the rapid degradation of interfacial materials in harsh conditions (*e.g.* low temperature and scratching), but also endowed the device with exceptional optical transparency and self-cleaning capabilities. Moreover, the tribo-motion between water droplets and the lubricant also yielded significant improvements in the charge transfer due to an increased contact area and prolonged contact time, which further enhanced the overall output performance of the device.

In view of these unique advantages of all-fluid-based TENGs, a plethora of intriguing applications have been proposed. For example, Niu et al. presented a liquid-liquid TENG to harness raindrop energy by guiding the droplets through a freely suspended liquid membrane (Figure 13c).[10] The liquid membrane was pre-charged by a negatively charged fluorinated ethylene propylene film through electrostatic induction. As the droplets traversed this liquid membrane, some of the charges were either absorbed or neutralized by the droplets, resulting in a charge redistribution on the membrane and consequent generation of current signals. This liquid membrane-based TENG demonstrated significant promise in various electronic applications, such as permeable sensors or charge filters. Moreover, the potential scope of this technology could be extended beyond raindrops, as it could be adapted to capture energy from fine particles and microfluidics.

This article is protected by copyright. All rights reserved.

Accepted Article

15214095, ja, Downloaded from https://onlinelibrary.wiley.com/doi/10.1002/adma.202308197 by Nanyang Technological University Lee Kong Chian School Of Medicine, Wiley Online Library on [16/10/2023]. See the Terms and Conditions (https://onlinelibrary.wiley.com/terms-and-conditions) on Wiley Online Library for rules of use; OA articles are governed by the applicable Creative Commons License

All-fluid-based TENGs also exhibit immense promise for applications in implantable devices. An innovative aqueous two-phase (polyethylene glycol-dextran, PEG-DEX) TENG has been developed, exhibiting outstanding biocompatibility and charge transfer efficiency.[16] As illustrated in Figure 13d (i), the physicochemical properties of bull serum albumin were preserved both within the PEG droplet and throughout the contact-separation process, indicating the excellent biocompatibility of this liquid-liquid TENG. The cytocompatibility assessment using a living/dead assay also revealed that the PEG-DEX system sustained approximately 95.14% cell viability during stable cell culture (Figure 13d (ii)). Furthermore, the teicoplanin-loaded aqueous PEG-DEX system exhibited excellent antibacterial properties (Figure 13d (iii)), accentuating its potential as a viable drug delivery system for living organisms. This pioneering advancement opened up new possibilities for the integration of TENG technology into implantable electronic devices, fostering the exciting prospect of self-powered sensors and sustainable power generation within the domain of biomedical applications.

This article is protected by copyright. All rights reserved.

Accepted Article

15214095, ja, Downloaded from https://onlinelibrary.wiley.com/doi/10.1002/adma.202308197 by Nanyang Technological University Lee Kong Chian School Of Medicine, Wiley Online Library on [16/10/2023]. See the Terms and Conditions (https://onlinelibrary.wiley.com/terms-and-conditions) on Wiley Online Library for rules of use; OA articles are governed by the applicable Creative Commons License

Accepted Article

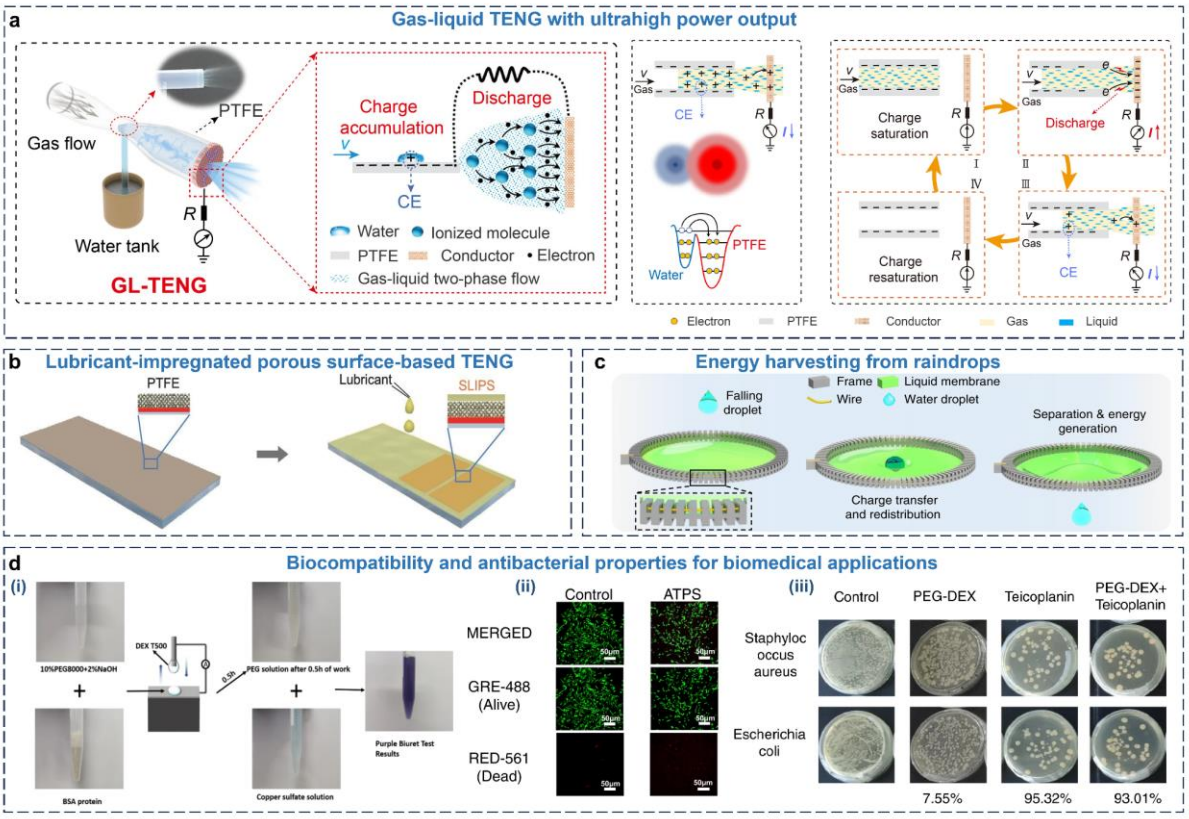

Figure 13. Advantages and possible applications for all-fluid-based TENGs. a) Schematic and working principle of gas-liquid two-phase flow-based TENG with ultrahigh power output. Reproduced with permission.[17] Copyright 2022, AAAS. b) Schematic of slippery lubricant-impregnated porous surface-based TENG with self-cleaning ability and excellent stability in harsh environments. Reproduced with permission.[80] Copyright 2019, Oxford University Press. c) Schematic diagram of energy harvesting from falling droplets based on liquid membrane TENG. Reproduced with permission.[10] Copyright 2019, Springer Nature. d) Superior biocompatibility and antibacterial properties of the aqueous PEG-DEX two-phase system TENG for biomedical applications. Reproduced with permission.[16] Copyright 2022, Springer Nature.

5. Theoretical and Simulation Analysis

5.1. Theoretical Model

This article is protected by copyright. All rights reserved.

15214095, ja, Downloaded from https://onlinelibrary.wiley.com/doi/10.1002/adma.202308197 by Nanyang Technological University Lee Kong Chian School Of Medicine, Wiley Online Library on [16/10/2023]. See the Terms and Conditions (https://onlinelibrary.wiley.com/terms-and-conditions) on Wiley Online Library for rules of use; OA articles are governed by the applicable Creative Commons License

Accepted Article

The development of a theoretical framework holds significant promise in advancing the comprehension of the operational principles of various FB-TENGs. In the context of liquid-based TENGs, the theoretical model is rooted in the phenomena of interfacial contact electrification and subsequent ion transfer processes, collectively conceptualized as a two-step electric double layer (EDL) formation model.[81] Taking liquid-solid TENG as an example, this two-step EDL formation process is depicted in **Figure 14a** (i). In the first step, electrons are transferred from the liquid molecules to the solid substrate upon contact, owing to the overlap of their electron clouds. Simultaneously, ionization reactions may occur on the solid surface, resulting in the generation of both electrons and ions at the solid-liquid interface. Consequently, the first layer of electrostatic charges will form at the solid surface. In the ensuing step, the oppositely charged ions within the liquid are drawn toward the charged surface through electrostatic attraction, culminating in the formation of an ion gradient proximate to the interface. This phenomenon subsequently gives rise to the creation of the EDL.[14] This two-step EDL model emphasizes the coexistence of electron exchange and ion adsorption.

Figure 14a (ii) provides empirical validation for this theoretical model. By recording the decay of contact electrification charges on diverse solid surfaces, it becomes feasible to isolate the individual contributions of electron transfer and ion transfer processes, respectively. The outcomes reveal that all charge decay curves align with the electron thermionic emission model.[82-83] This finding implies that the "sticky" charges originate from ion adsorption, whereas the mobile charges are contributed by electron transfer. From the results, the ratio between the electron and ion transfer for liquid-solid TENGs highly depends on the physicochemical characteristics of both the solid materials and the liquids involved, as well as their contact electrification.

This article is protected by copyright. All rights reserved.

15214095, ja, Downloaded from https://onlinelibrary.wiley.com/doi/10.1002/adma.202308197 by Nanyang Technological University Lee Kong Chian School Of Medicine, Wiley Online Library on [16/10/2023]. See the Terms and Conditions (https://onlinelibrary.wiley.com/terms-and-conditions) on Wiley Online Library for rules of use; OA articles are governed by the applicable Creative Commons License

Accepted Article

Building upon the two-step EDL formation process, an equivalent circuit model and its corresponding mathematical equations are also investigated to explicate the working mechanism of liquid-solid TENGs. Figure 14b displays a typical structure of liquid-solid TENG, comprising dielectric materials (Kapton and PTFE), liquid medium (deionized water), and two electrodes. The whole device can be represented by an equivalent circuit model through a series connection of two capacitors and a water resistor.[84] Specifically, one capacitor is distributed at the interface between the liquid and solid surface, while the other one is situated at the surface of the submerged electrode. Based on this model, the corresponding electric outputs, including open-circuit voltage $\boldsymbol{V_{OC}(t)}$, short-circuit transferred charges $\boldsymbol{Q_{SC}(t)}$ and total capacitance $\boldsymbol{C_{(t)}}$, can be quantitatively predicted by the following formula:

$$\boldsymbol{V_{OC}(t) = \frac{S_b \sigma_b}{C_{bot}} - \frac{\sigma_w d_0}{S_w}} \quad (1)$$

$$\boldsymbol{Q_{SC}(t) = \frac{S_b \sigma_b - \sigma_w d_0 C_{bot}/\varepsilon_0}{1 + C_{bot}/C_{top}}} \quad (2)$$

$$\boldsymbol{C_{(t)} = \frac{\varepsilon_0 \varepsilon_w}{\lambda_w / S_b + d_0 \varepsilon_w / S_w}} \quad (3)$$

Where $\boldsymbol{S_b}$ and $\boldsymbol{S_w}$ represent the contact area between the liquid and the bottom electrode and the contact area between the liquid and dielectric material; $\boldsymbol{\sigma_b}$ and $\boldsymbol{\sigma_w}$ are the charge density distributed at the surface of the bottom electrode and liquid-dielectric material, respectively; $\boldsymbol{d_0}$ is the effective thickness of the dielectric layer; $\boldsymbol{\varepsilon_0}$ and $\boldsymbol{\varepsilon_w}$ are permittivity of vacuum and relative permittivity of the dielectric materials; $\boldsymbol{\lambda_w}$ is the width of the EDL capacitor; $\boldsymbol{C_{bot}}$ is the capacitance of the EDL capacitor formed at the liquid-bottom electrode interface; $\boldsymbol{C_{top}}$ represents the

This article is protected by copyright. All rights reserved.

15214095, ja, Downloaded from https://onlinelibrary.wiley.com/doi/10.1002/adma.202308197 by Nanyang Technological University Lee Kong Chian School Of Medicine, Wiley Online Library on [16/10/2023]. See the Terms and Conditions (https://onlinelibrary.wiley.com/terms-and-conditions) on Wiley Online Library for rules of use; OA articles are governed by the applicable Creative Commons License

combination of the EDL capacitance formed at the water-solid interface and the time-invariant capacitance caused by dielectric material.

This two-step EDL theory can also be applied to elucidate the charge transfer process of liquid-liquid TENGs. Taking the oil-water system as an example (Figure 14c)[77], water droplets descend within an oil-filled container, resulting in molecular or ionic collisions at the interface between the two immiscible liquids. During this dynamic process, the interfacial friction energy serves as the driving force, exciting both electronic transitions and ionic reactions, thereby engendering a substantial influx of ions and electrons. Subsequently, negative ions within the aqueous solution are propelled toward the interface due to electrostatic interactions, ultimately culminating in the formation of the EDL at the liquid-liquid interface.

This article is protected by copyright. All rights reserved.

Accepted Article

15214095, ja, Downloaded from https://onlinelibrary.wiley.com/doi/10.1002/adma.202308197 by Nanyang Technological University Lee Kong Chian School Of Medicine, Wiley Online Library on [16/10/2023]. See the Terms and Conditions (https://onlinelibrary.wiley.com/terms-and-conditions) on Wiley Online Library for rules of use; OA articles are governed by the applicable Creative Commons License

Accepted Article

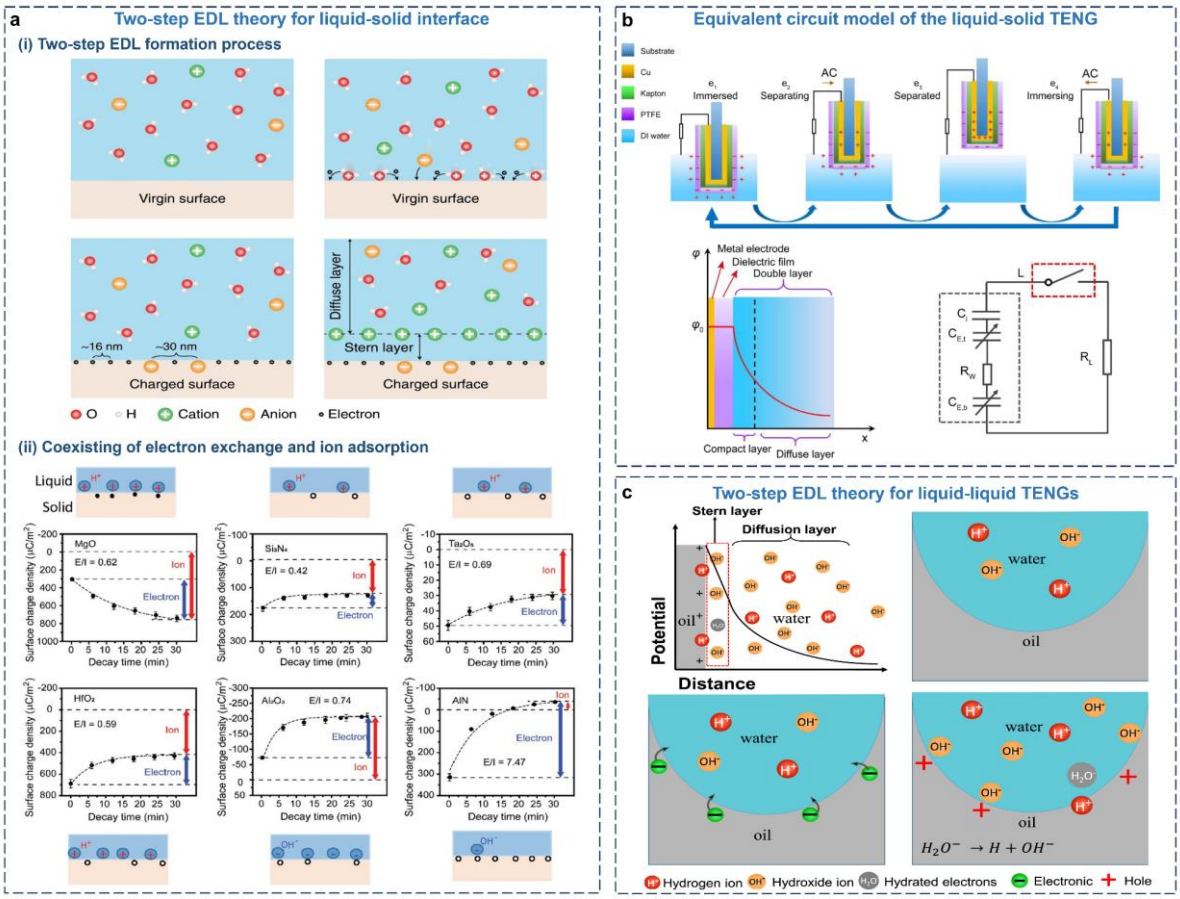

Figure 14. Theoretical models for working mechanism of liquid-based FB-TENGs. a) Two-step EDL theory for a liquid-solid interface: (i) The two-step EDL formation process for a liquid-solid TENG. (ii) Coexisting of electron exchange and ion adsorption for various liquid-solid interfaces. Reproduced with permission.[14] Copyright 2020, Springer Nature. b) Equivalent circuit model for liquid-solid TENG. Reproduced with permission.[84] Copyright 2021, American Chemical Society. c) Two-step EDL theory for liquid-liquid TENGs. Reproduced with permission.[77] Copyright 2021, Elsevier.

Although promising progresses have been made in liquid-based TENGs, the theoretical investigation and mathematical model for gas-involved interfacial systems are still rare. It is hypothesized that electron transfer still dominated the charge generation mechanism when the gas impacted the liquid or solid surface to induce the electron clouds overlapping.[81] One interesting

This article is protected by copyright. All rights reserved.

15214095, ja, Downloaded from https://onlinelibrary.wiley.com/doi/10.1002/adma.202308197 by Nanyang Technological University Lee Kong Chian School Of Medicine, Wiley Online Library on [16/10/2023]. See the Terms and Conditions (https://onlinelibrary.wiley.com/terms-and-conditions) on Wiley Online Library for rules of use; OA articles are governed by the applicable Creative Commons License

example to support this hypothesis is the phenomenon of the negatively charged raindrops in nature. During the falling process of the raindrops, a strong interfacial friction would occur between the air and raindrops and the electrons would transfer from the air to the rain, leading to the negatively charged raindrops. However, a systematic and comprehensive theoretical investigation is still lacking in mechanical energy harvesters based on gas-involved interface, which demands more efforts to complete the theoretical framework for various types of FB-TENGs.

5.2. Simulation Analysis

To gain a more comprehensive understanding of the charge transfer process in FB-TENGs, diverse simulation processes, such as interactive dynamics between fluids and the electric field distribution, have been conducted to explore various impact factors on the contact electrification at the fluid interface. As an example of fluid dynamics simulation, the contact electrification between PTFE and gas has been systematically investigated from both experimental and simulation aspects, as illustrated in **Figures 15**a and 15b.[85] During the falling process of the PTFE ball, the bottom surface of the solid was in a compression state on account of its intense collision with gas molecules. Consequently, the pressure difference formed around the solid would drive strong friction and contact electrification between the gas molecules and the solid, as demonstrated in the simulation analysis in Figures 15c and 15d. The experiment results from the gas-solid contact electrification also corresponded well with the simulation, indicating the surface area and falling velocity of the solid would dramatically affect the charge transfer process at the gas-solid interface.

To better understand the contact electrification process of FB-TENGs, a finite element analysis tool was also adopted to simulate the electric field distribution at the fluid interface, as displayed in

This article is protected by copyright. All rights reserved.

Accepted Article

15214095, ja, Downloaded from https://onlinelibrary.wiley.com/doi/10.1002/adma.202308197 by Nanyang Technological University Lee Kong Chian School Of Medicine, Wiley Online Library on [16/10/2023]. See the Terms and Conditions (https://onlinelibrary.wiley.com/terms-and-conditions) on Wiley Online Library for rules of use; OA articles are governed by the applicable Creative Commons License

Figures 15e and 15f.[16] According to the fundamental theory of TENGs[86], the relationship among the displacement field (*D*), surface charge density (*ρ*) and electric field (*E*) could be described as follows when there was no magnetic field:

$$\nabla \cdot \boldsymbol{D} = \boldsymbol{\rho} \quad (1)$$

$$\boldsymbol{D} = \boldsymbol{\varepsilon_r \varepsilon_0 E} \quad (2)$$

$$\boldsymbol{E} = -\nabla \varphi \quad (3)$$

where $\boldsymbol{\varepsilon_r}$ and $\boldsymbol{\varepsilon_0}$ were the dielectric constant of the dielectric material and vacuum, respectively; φ represented the electrical potential. Hence, the relationship between φ and ρ could be described as follows:

$$-\boldsymbol{\varepsilon_r \varepsilon_0} \nabla^2 \varphi = \boldsymbol{\rho} \quad (4)$$

Utilizing the formulas presented above, it is feasible to conduct simulations for the stationary space potential, transferred charge, and induced current. As an illustration, the electric potential exhibits an augmentation in response to an increase in the gap distance between two immiscible droplets, as represented in Figures 15e and 15f. Similarly, the transferred charge and output current could also be obtained by simulating the contact-separation process of two fluids (Figure 15g and 15h).

This article is protected by copyright. All rights reserved.

Accepted Article

15214095, ja, Downloaded from https://onlinelibrary.wiley.com/doi/10.1002/adma.202308197 by Nanyang Technological University Lee Kong Chian School Of Medicine, Wiley Online Library on [16/10/2023]. See the Terms and Conditions (https://onlinelibrary.wiley.com/terms-and-conditions) on Wiley Online Library for rules of use; OA articles are governed by the applicable Creative Commons License

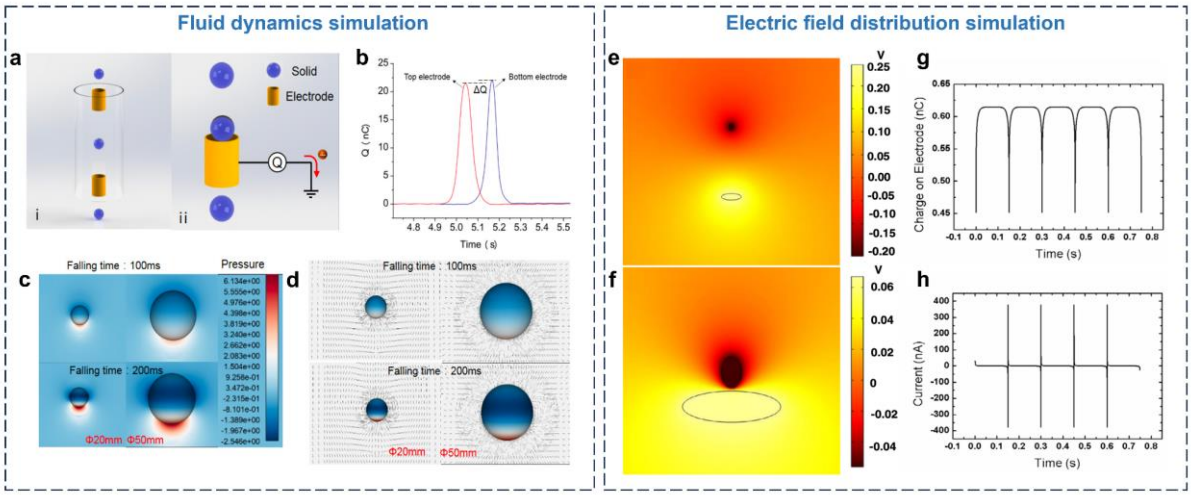

Figure 15. Simulations of fluid dynamics and electric field distribution for FB-TENGs. a) Schematic illustration of the working mechanism for gas-solid contact electrification. b) The transferred charge detected by the top and bottom electrodes. c) The simulation of the pressure change around the solid under different surface areas and velocities. d) The gas distribution simulation around the solid under different surface areas and velocities. Reproduced with permission.[85] Copyright 2023, MDPI. Electric field distribution simulation for liquid-liquid TENGs, from far distance (e) to the contact interface (f). The transferred charge (g) and output current on the electrode over time (h). Reproduced with permission.[16] Copyright 2022, Springer Nature.

Various simulation methods offer valuable means for elucidating the intricacies of charge transfer mechanisms across different fluid systems. However, it is noteworthy that existing simulations predominantly rely on rudimentary models, largely neglecting essential elements such as surface morphology, fluidic properties and contact-separation efficiency between two different fluids. For the future trajectory of the simulation analysis, it is paramount to develop a more encompassing model. This advanced model should incorporate the aforementioned influential factors, thus

This article is protected by copyright. All rights reserved.

Accepted Article

15214095, ja, Downloaded from https://onlinelibrary.wiley.com/doi/10.1002/adma.202308197 by Nanyang Technological University Lee Kong Chian School Of Medicine, Wiley Online Library on [16/10/2023]. See the Terms and Conditions (https://onlinelibrary.wiley.com/terms-and-conditions) on Wiley Online Library for rules of use; OA articles are governed by the applicable Creative Commons License

furnishing a precise and systematic framework for capturing the significant characteristics of contact electrification at fluid interfaces.

Table 1. Summary of the materials and the electric performance of various FB-TENGs.

Materials	Type	Voltage	Current	Power	Charge transfer	Refs.
Water/pyramid PDMS	L-S[a)]	52 V	2.45 mA m^{-2}	0.13 W m^{-2}	31.3 μC m^{-2}	[8]
Water/nanostructured PTFE	L-S	9.3 V	10.63 mA m^{-2}	0.091 W m^{-2}	0.69 μC m^{-2}	[9]
Water/FEP	L-S	160 V	1.73 mA m^{-2}	0.067 W m^{-2}	41.7 μC m^{-2}	[30]
Water/PTFE	L-S	400 V	5 mA m^{-2}	-	125 μC m^{-2}	[35]
Water/HCOENPs[b)]-coated PET fabric	L-S	22 V	35.6 mA m^{-2}	0.30 W m^{-2}	-	[40]
Water/CYTOP[c)]	L-S	132 V	30 μA	1 mW	-	[41]
Water/FEVE[d)]	L-S	80 V	5 mA m^{-2}	0.089 W m^{-2}	-	[50]
Water/PTFE	L-S	143.5 V	300 mA m^{-2}	50.1 W m^{-2}	59.2 μC m^{-2}	[12]
Water/PTFE nanowires	L-S	300 V	0.19 mA m^{-2}	0.015 W m^{-2}	30 μC m^{-2}	[38]

This article is protected by copyright. All rights reserved.

Accepted Article

15214095, ja, Downloaded from https://onlinelibrary.wiley.com/doi/10.1002/adma.202308197 by Nanyang Technological University Lee Kong Chian School Of Medicine, Wiley Online Library on [16/10/2023]. See the Terms and Conditions (https://onlinelibrary.wiley.com/terms-and-conditions) on Wiley Online Library for rules of use; OA articles are governed by the applicable Creative Commons License

Water/FEP	L-S	228 V	11.5 μA	3.7 mW	-	[11]
Silicone oil/Nylon	L-S	4600 V	138 mA m^{-2}	19.48 W m^{-2}	4660 μC m^{-2}	[19]
Parffin oil-water/PTFE-PDA[e)]	L-S	15 V	0.012 mA m^{-2}	-	-	[54]
Liquid chemicals/PTFE	L-S	0.116 V	0.0018 mA m^{-2}	-	-	[87]
liquid metal mercury/PVDF	L-S	15.5 V	300 nA	-	-	[88]
PFDTS[f)] modified ITO/$K_3[Fe(CN)_6]$-$K_4[Fe(CN)_6]$	L-S	8 mV	-	-	-	[89]
Water/PTFE nanoparticles	L-S	230 V	13 μA	1.1 mW	-	[56]
Water/Teflon-coated ITO	L-S	50 V	-	-	-	[90]
H_2SO_4/PTFE filament	L-S	0.025 V	0.02 nA	-	-	[91]
Water/Fluoropolymer	L-S	400 V	2 mA m^{-2}	162 W m^{-2}	~22 nC	[23]
Water/PTFE	L-S	344 V	2.3 mA m^{-2}	2030 W m^{-2}	~13 nC	[24]
Water/FEP	L-S	~600 V	1.72 mA	48.7 kW m^{-2}	-	[25]

This article is protected by copyright. All rights reserved.

Accepted Article

15214095, ja, Downloaded from https://onlinelibrary.wiley.com/doi/10.1002/adma.202308197 by Nanyang Technological University Lee Kong Chian School Of Medicine, Wiley Online Library on [16/10/2023]. See the Terms and Conditions (https://onlinelibrary.wiley.com/terms-and-conditions) on Wiley Online Library for rules of use; OA articles are governed by the applicable Creative Commons License

Water/Slippery lubricant	L-S	100 V	1.5 mA	118 W m^{-2}	-	[26]
Seawater/FEP	L-S	78 V	70 nA	-	300 nC	[27]
DI water/FEP	L-S	210 V	268 nA	-	742 nC	[27]
DI water/FEP	L-S	77 V	52 nA	23.3 μW	30.7 nC	[28]
Water/FEP	L-S	96 V	6.86 μA	1.98 W m^{-2}	17.8 nC	[43]
Water/Polyfluoroalkoxy	L-S	511 V	2.28 mA	26.6 mW	-	[46]
Air bubble/PTFE	G-S[g)]	~35 mV	-	-	-	[73]
Air/PDPU[h)]	G-S	5.2 V	0.5 mA m^{-2}	-	27 nC	[13]
Air bubble/PTFE	G-S	3 V	~40 nA		~2.2 nC	[71]
Air bubble/PTFE	G-S	40.3 V	2.4 μA	56.4 W m^{-3}	~20 nC	[18]
Air bubble/PTFE	G-S	17.5 V	-	-	-	[72]
Water/Sugar-SDS[i)]-PVA[j)] liquid membrane	L-L[k)]	4V	60 nA	137.4 nW	1 nC	[10]
Water/Lubricant oil	L-L	5V	400 nA	200 nW	3 nC	[80]

This article is protected by copyright. All rights reserved.

Accepted Article

15214095, ja, Downloaded from https://onlinelibrary.wiley.com/doi/10.1002/adma.202308197 by Nanyang Technological University Lee Kong Chian School Of Medicine, Wiley Online Library on [16/10/2023]. See the Terms and Conditions (https://onlinelibrary.wiley.com/terms-and-conditions) on Wiley Online Library for rules of use; OA articles are governed by the applicable Creative Commons License

Accepted Article

Ferrofluid/ Lubricant oil	L-L	-	0.178 nA	-	-	[75]
PEG[l)]/DEX[m)]	L-L	0.47 V	720 nA	100 nW	1 mC m^{-2}	[16]
Air/Water discharging	G-L[n)]	3789 V	867 μA	143.6 kW m^{-3}	859 mC m^{-3}	[17]

[a)]L-S: Liquid-solid TENG; [b)]HCOENPs: Hydrophobic cellulose oleoyl ester nanoparticles; [c)]CYTOP: Cyclized transparent optical polymer; [d)]FEVE: Fluoroolefin-vinyl ether; [e)]PDA: Polydopamine; [f)]PFDTS: Perfluorodecyltriethoxysilane; [g)]G-S: Gas-solid TENG; [h)]PDPU: Polysiloxane-dimethylglyoxime–based polyurethane; [i)]SDS: Sodium dodecyl sulfate; [j)]PVA: Polyvinyl alcohol; [k)]L-L: Liquid-liquid TENG; [l)]PEG: Polyethylene glycol; [m)]DEX: Dextran; [n)]G-L: Gas-liquid TENGs.

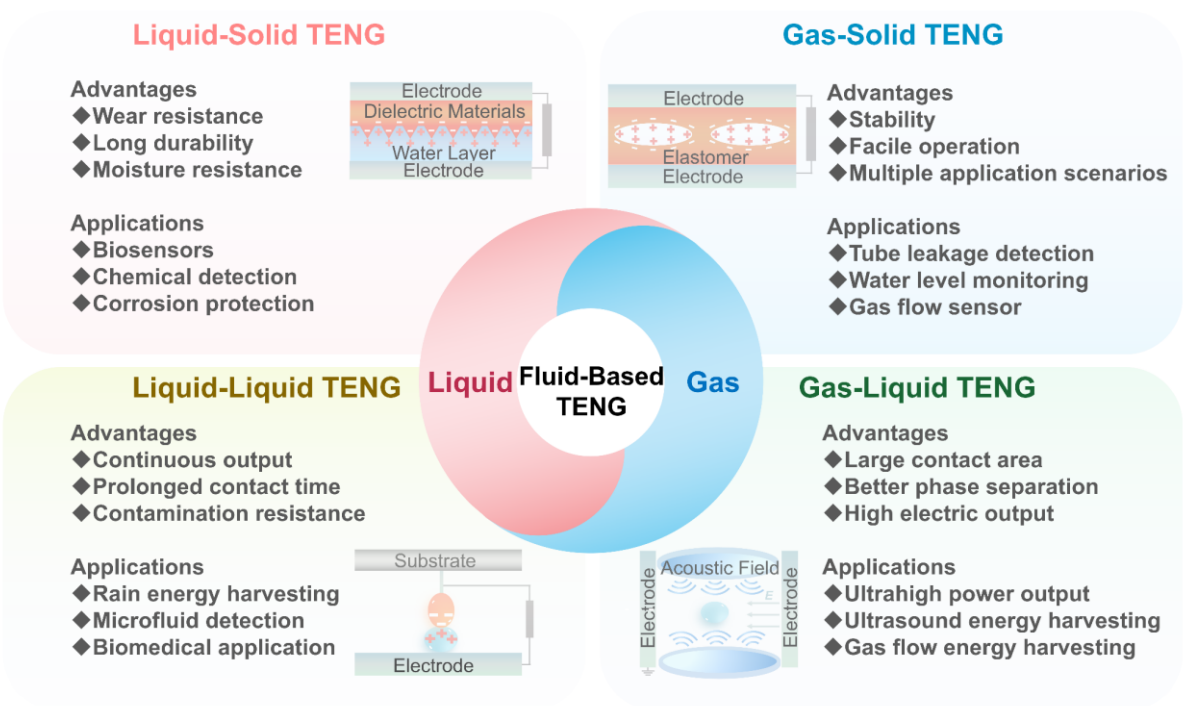

This article is protected by copyright. All rights reserved.

15214095, ja, Downloaded from https://onlinelibrary.wiley.com/doi/10.1002/adma.202308197 by Nanyang Technological University Lee Kong Chian School Of Medicine, Wiley Online Library on [16/10/2023]. See the Terms and Conditions (https://onlinelibrary.wiley.com/terms-and-conditions) on Wiley Online Library for rules of use; OA articles are governed by the applicable Creative Commons License

Figure 16. A summary of advantages and applications of various fluid-based TENGs.

6. Conclusions and Perspectives

In conclusion, FB-TENGs have emerged as promising energy harvesters, effectively addressing the intrinsic limitations encountered by all-solid TENGs, including wear abrasion and limited effective contact area. By harnessing the dynamic and continuous characteristics of fluids, FB-TENGs facilitate an enhanced contact area and improved energy conversion efficiency, thus unlocking a myriad of application scenarios ranging from biomedical sensors to distributed energy systems. As a summary, different materials, output performance, advantages and applications of various FB-TENGs are provided in Table 1 and **Figure 16**. Despite their enticing properties and diverse applications, the intricate interfacial interactions and precise fluid manipulation present challenges for various types of FB-TENGs.

Liquid-solid TENGs have displayed a multitude of advantages, such as performance stability, operational durability and self-cleaning capacity, but they also come with their challenges in comparison to all-solid-based TENGs. On one hand, the integration of liquid medium into the TENG may complicate the device fabrication and encapsulation process, posing challenges for large-scale energy harvesting applications. On the other hand, the selection of suitable liquids is still limited because numerous factors need to be considered, including the power output, chemical compatibility with solid materials, potential safety risk, as well as performance stability over prolonged use. Despite these challenges, new opportunities also come along with application innovation and expansion. For example, some biofluids, such as sweat and blood, can be directly utilized for triboelectric materials, which can sense various bio-signals (*e.g.* ion type and

This article is protected by copyright. All rights reserved.

Accepted Article

15214095, ja, Downloaded from https://onlinelibrary.wiley.com/doi/10.1002/adma.202308197 by Nanyang Technological University Lee Kong Chian School Of Medicine, Wiley Online Library on [16/10/2023]. See the Terms and Conditions (https://onlinelibrary.wiley.com/terms-and-conditions) on Wiley Online Library for rules of use; OA articles are governed by the applicable Creative Commons License

concentration, pH value and fluid flow speed), opening up new possibilities for biomedical applications. Furthermore, the abundant energy sources from the ocean, such as wave energy, current energy and tidal energy, provide an ideal application scenario for liquid-solid TENGs, allowing them to transform mechanical energy into electricity without additional energy conversion steps and to possess massive and infinite energy input source.

For gas-solid TENGs, some new materials and structures beyond the porous elastomer and bubble-based configurations should also be investigated to address the existing challenges including low energy density, gas leakage risk, intricate gas flow control, and limited contact area between gas and solid. Some promising fabrication techniques, such as additive manufacturing and micro-/nano-processing, can also be adopted to engineer the pore structure of the elastomer and manipulate the surface patterns of dielectric materials, further promoting the output performance and user-friendliness of the device. A critical aspect that requires urgent attention pertains to the lack of mechanism validation and theoretical models in the realm of gas-solid TENGs. Addressing this deficiency necessitates concerted efforts to advance our understanding and fill this knowledge gap, thereby fostering the acceleration of innovation and development in this emerging field.

Regarding all-fluid-based TENGs, the prevailing focus has predominantly centered on water or air-based systems due to their versatile applicability and ease of operation. However, it is essential to recognize the urgency in broadening the scope of liquid and gas materials considered. This imperative arises not solely from the pursuit of achieving higher power outputs but also from the desire to gain a comprehensive understanding of the intricate charge transfer mechanisms occurring at fluid interfaces. The complex rheological properties inherent in fluids pose another significant challenge that necessitates resolution. To solve this challenge, realizing an effective interfacial

This article is protected by copyright. All rights reserved.

Accepted Article

15214095, ja, Downloaded from https://onlinelibrary.wiley.com/doi/10.1002/adma.202308197 by Nanyang Technological University Lee Kong Chian School Of Medicine, Wiley Online Library on [16/10/2023]. See the Terms and Conditions (https://onlinelibrary.wiley.com/terms-and-conditions) on Wiley Online Library for rules of use; OA articles are governed by the applicable Creative Commons License

control is necessary to improve contact-separation efficiency and extend the applicability of FB-TENGs to a broader array of scenarios. Therefore, further exploration is essential to identify more controllable approaches apart from the acoustic levitation technique and Venturi-like structural design. This pursuit aims to establish a more convenient and universally applicable approach for fabricating all-fluid-based TENGs.

While numerous materials and structural configurations have been devised to achieve enhanced output performance of various FB-TENGs, it is also imperative to underscore their long-term reliability, considering their susceptibility to a multitude of factors. Fluid properties, such as viscosity and wettability, stand out as crucial factors influencing the operational stability of FB-TENGs. On one hand, high-viscosity fluids can enhance friction and prolong contact time between triboelectric materials, resulting in improved charge transfer and increased electric output. Nevertheless, excessively high viscosity can diminish contact-separation efficiency and lead to excessive wear between fluids and solids, negatively impacting continuous power generation and device durability. On the other hand, maintaining suitable wettability is critical to ensure a robust and consistent interaction between fluids and solids. Solids with high hydrophobicity promote contact-separation efficiency at the interface, preventing liquid residue on solid surfaces, thus ensuring a stable contact area and sustained output performance for fluid-based energy harvesters. Contamination poses another concern for the long-term stability of FB-TENGs, as fluids exposed to the environment may absorb dust, dirt, and suspended particles. These contaminants may alter the physicochemical properties of the fluids or accumulate on solid surfaces, potentially affecting the output performance of FB-TENGs. Potential solutions to mitigate this issue include the development of self-cleaning materials or the implementation of effective encapsulation for the entire device. Electrode

This article is protected by copyright. All rights reserved.

Accepted Article

15214095, ja, Downloaded from https://onlinelibrary.wiley.com/doi/10.1002/adma.202308197 by Nanyang Technological University Lee Kong Chian School Of Medicine, Wiley Online Library on [16/10/2023]. See the Terms and Conditions (https://onlinelibrary.wiley.com/terms-and-conditions) on Wiley Online Library for rules of use; OA articles are governed by the applicable Creative Commons License

corrosion is another consideration for the durability of FB-TENGs. Depending on the fluid type, traditional metal electrodes like copper and aluminum may corrode over time due to different chemical or redox reactions. Therefore, selecting suitable electrode materials, such as carbon-based materials and conducting polymers, which are chemically stable in the chosen fluid environment, is critical to guarantee operational stability in FB-TENGs. Finally, environmental factors, such as temperature and humidity, also play a vital role in the charge transfer and dissipation process at the fluid interface, which affect the device performance and stability as well, so maintaining stable environmental conditions within the desired range is also a significant method to ensure the longevity and reliability of FB-TENGs.

Apart from the stability concerns of various FB-TENGs, the understanding of the dynamic behaviors and physicochemical properties at fluid-fluid and fluid-solid interfaces is also in the preliminary stage. The complex interfacial phenomena, such as capillary action, wetting, interfacial tension, as well as fluid flow and diffusion should be investigated to construct their relationship with charge generation and transfer efficiency of FB-TENGs, which can offer constructive guidance to enhance the device performance via fluid manipulation and structural design. Furthermore, the fundamentals including contact electrification, surface reactivity as well as fluid composition, still require substantial experimental measurements, theoretical modeling and simulation analysis to obtain deeper insights into diverse fluid interactions and their influence on the electric performance of energy harvesters.

Acknowledgements

This article is protected by copyright. All rights reserved.

Accepted Article

15214095, ja, Downloaded from https://onlinelibrary.wiley.com/doi/10.1002/adma.202308197 by Nanyang Technological University Lee Kong Chian School Of Medicine, Wiley Online Library on [16/10/2023]. See the Terms and Conditions (https://onlinelibrary.wiley.com/terms-and-conditions) on Wiley Online Library for rules of use; OA articles are governed by the applicable Creative Commons License

F. J., L. Z. and J. P. L. contributed equally to this work. This work was supported by the Ministry of Education (MOE) Singapore, AcRF Tier 1 (Award No. RT15/20). F. J. acknowledges the research scholarship awarded by the Institute of Flexible Electronics Technology of Tsinghua, Zhejiang (IFET-THU), Nanyang Technological University (NTU), and Qiantang Science and Technology Innovation Center, China (QSTIC).

Conflict of Interest

The authors declare no conflict of interest.

Received: ((will be filled in by the editorial staff))
Revised: ((will be filled in by the editorial staff))
Published online: ((will be filled in by the editorial staff))

References

[1] D. Choi, Y. Lee, Z.-H. Lin, S. Cho, M. Kim, C. K. Ao, S. Soh, C. Sohn, C. K. Jeong, J. Lee, M. Lee, S. Lee, J. Ryu, P. Parashar, Y. Cho, J. Ahn, I.-D. Kim, F. Jiang, P. S. Lee, G. Khandelwal, S.-J. Kim, H. S. Kim, H.-C. Song, M. Kim, J. Nah, W. Kim, H. G. Menge, Y. T. Park, W. Xu, J. Hao, H. Park, J.-H. Lee, D.-M. Lee, S.-W. Kim, J. Y. Park, H. Zhang, Y. Zi, R. Guo, J. Cheng, Z. Yang, Y. Xie, S. Lee, J. Chung, I.-K. Oh, J.-S. Kim, T. Cheng, Q. Gao, G. Cheng, G. Gu, M. Shim, J. Jung, C. Yun, C. Zhang, G. Liu, Y. Chen, S. Kim, X. Chen, J. Hu, X. Pu, Z. H. Guo, X. Wang, J. Chen, X. Xiao, X. Xie, M. Jarin, H. Zhang, Y.-C. Lai, T. He, H. Kim, I. Park, J. Ahn, N. D. Huynh, Y. Yang, Z. L. Wang, J. M. Baik, D. Choi, *ACS Nano* **2023**, *17*, 11087-11219.

[2] W.-G. Kim, D.-W. Kim, I.-W. Tcho, J.-K. Kim, M.-S. Kim, Y.-K. Choi, *ACS Nano* **2021**, *15*, 258-287.

[3] T. Cheng, J. Shao, Z. L. Wang, *Nat. Rev. Methods Primers* **2023**, *3*, 39.

This article is protected by copyright. All rights reserved.

Accepted Article

15214095, ja, Downloaded from https://onlinelibrary.wiley.com/doi/10.1002/adma.202308197 by Nanyang Technological University Lee Kong Chian School Of Medicine, Wiley Online Library on [16/10/2023]. See the Terms and Conditions (https://onlinelibrary.wiley.com/terms-and-conditions) on Wiley Online Library for rules of use; OA articles are governed by the applicable Creative Commons License

[4] R. Liu, Z. L. Wang, K. Fukuda, T. Someya, *Nat. Rev. Mater.* **2022**, *7*, 870-886.

[5] W. Zhang, Y. Shi, Y. Li, X. Chen, H. Shen, *Front. Mater.* **2022**, *9*, 909746.

[6] Z. Wang, Y. Wang, Q. Gao, G. Bao, T. Cheng, Z. L. Wang, *Adv. Mater. Technol.* **2023**, *8*, 2201029.

[7] Q.-T. Nguyen, K.-K. K. Ahn, *Int. J. Precis. Eng. Manuf. - Green Technol.* **2021**, *8*, 1043-1060.

[8] Z.-H. Lin, G. Cheng, L. Lin, S. Lee, Z. L. Wang, *Angew. Chem. Int. Ed.* **2013**, *52*, 12545-12549.

[9] Z.-H. Lin, G. Cheng, S. Lee, K. C. Pradel, Z. L. Wang, *Adv. Mater.* **2014**, *26*, 4690-4696.

[10] J. Nie, Z. Wang, Z. Ren, S. Li, X. Chen, Z. Lin Wang, *Nat. Commun.* **2019**, *10*, 2264.

[11] J. Wang, Z. Wu, L. Pan, R. Gao, B. Zhang, L. Yang, H. Guo, R. Liao, Z. L. Wang, *ACS Nano* **2019**, *13*, 2587-2598.

[12] W. Xu, H. Zheng, Y. Liu, X. Zhou, C. Zhang, Y. Song, X. Deng, M. Leung, Z. Yang, R. X. Xu, Z. L. Wang, X. C. Zeng, Z. Wang, *Nature* **2020**, *578*, 392-396.

[13] J. Xiong, G. Thangavel, J. Wang, X. Zhou, P. S. Lee, *Sci. Adv.* **2020**, *6*, eabb4246.

[14] S. Lin, L. Xu, A. Chi Wang, Z. L. Wang, *Nat. Commun.* **2020**, *11*, 399.

[15] Z. Tang, S. Lin, Z. L. Wang, *Adv. Mater.* **2021**, *33*, 2102886.

[16] Y. Lu, L. Jiang, Y. Yu, D. Wang, W. Sun, Y. Liu, J. Yu, J. Zhang, K. Wang, H. Hu, X. Wang, Q. Ma, X. Wang, *Nat. Commun.* **2022**, *13*, 5316.

[17] Y. Dong, S. Xu, C. Zhang, L. Zhang, D. Wang, Y. Xie, N. Luo, Y. Feng, N. Wang, M. Feng, X. Zhang, F. Zhou, Z. L. Wang, *Sci. Adv.* **2022**, *8*, eadd0464.

[18] X. Yan, W. Xu, Y. Deng, C. Zhang, H. Zheng, S. Yang, Y. Song, P. Li, X. Xu, Y. Hu, L. Zhang, Z. Yang, S. Wang, Z. Wang, *Sci. Adv.* **2022**, *8*, eabo7698.

[19] W. He, C. Shan, S. Fu, H. Wu, J. Wang, Q. Mu, G. Li, C. Hu, *Adv. Mater.* **2023**, *35*, 2209657.

[20] F.-R. Fan, Z.-Q. Tian, Z. Lin Wang, *Nano Energy* **2012**, *1*, 328-334.

[21] V. Nguyen, R. Yang, *Nano Energy* **2013**, *2*, 604-608.

[22] F. Galembeck, T. A. L. Burgo, L. B. S. Balestrin, R. F. Gouveia, C. A. Silva, A. Galembeck, *RSC Adv.* **2014**, *4*, 64280-64298.

[23] H. Wu, N. Mendel, S. van der Ham, L. Shui, G. Zhou, F. Mugele, *Adv. Mater.* **2020**, *32*, 2001699.

This article is protected by copyright. All rights reserved.

Accepted Article

15214095, ja, Downloaded from https://onlinelibrary.wiley.com/doi/10.1002/adma.202308197 by Nanyang Technological University Lee Kong Chian School Of Medicine, Wiley Online Library on [16/10/2023]. See the Terms and Conditions (https://onlinelibrary.wiley.com/terms-and-conditions) on Wiley Online Library for rules of use; OA articles are governed by the applicable Creative Commons License

[24] N. Zhang, H. Zhang, W. Xu, H. Gu, S. Ye, H. Zheng, Y. Song, Z. Wang, X. Zhou, *Droplet* **2022**, *1*, 56-64.

[25] M. Liao, W. Xu, Y. Song, Z. Pan, H. Zheng, Y. Li, X. Qin, L. Wang, J. Lu, Z. Wang, *Nano Energy* **2023**, *116*, 108831.

[26] Y. Song, W. Xu, Y. Liu, H. Zheng, M. Cui, Y. Zhou, B. Zhang, X. Yan, L. Wang, P. Li, X. Xu, Z. Yang, Z. Wang, *Innovation* **2022**, *3*.

[27] C. Zhang, B. Zhang, W. Yuan, O. Yang, Y. Liu, L. He, Z. Zhao, L. Zhou, J. Wang, Z. L. Wang, *ACS Appl. Mater. Interfaces* **2022**, *14*, 8605-8612.

[28] X. Wei, Z. Zhao, C. Zhang, W. Yuan, Z. Wu, J. Wang, Z. L. Wang, *ACS Nano* **2021**, *15*, 13200-13208.

[29] T. Zhao, M. Xu, X. Xiao, Y. Ma, Z. Li, Z. L. Wang, *Nano Energy* **2021**, *88*, 106199.

[30] G. Zhu, Y. Su, P. Bai, J. Chen, Q. Jing, W. Yang, Z. L. Wang, *ACS Nano* **2014**, *8*, 6031-6037.

[31] Y. Jin, C. Wu, P. Sun, M. Wang, M. Cui, C. Zhang, Z. Wang, *Droplet* **2022**, *1*, 92-109.

[32] D. J. Lacks, T. Shinbrot, *Nat. Rev. Chem.* **2019**, *3*, 465-476.

[33] J. Nie, Z. Ren, L. Xu, S. Lin, F. Zhan, X. Chen, Z. L. Wang, *Adv. Mater.* **2020**, *32*, 1905696.

[34] Y. Nan, J. Shao, M. Willatzen, Z. L. Wang, *Research* **2022**, *2022*.

[35] X. Li, J. Tao, X. Wang, J. Zhu, C. Pan, Z. L. Wang, *Adv. Energy Mater.* **2018**, *8*, 1800705.

[36] D. Yoo, S.-C. Park, S. Lee, J.-Y. Sim, I. Song, D. Choi, H. Lim, D. S. Kim, *Nano Energy* **2019**, *57*, 424-431.

[37] D. Choi, D. W. Kim, D. Yoo, K. J. Cha, M. La, D. S. Kim, *Nano Energy* **2017**, *36*, 250-259.

[38] X. J. Zhao, S. Y. Kuang, Z. L. Wang, G. Zhu, *ACS Nano* **2018**, *12*, 4280-4285.

[39] X. Li, L. Zhang, Y. Feng, X. Zhang, D. Wang, F. Zhou, *Adv. Funct. Mater.* **2019**, *29*, 1903587.

[40] J. Xiong, M.-F. Lin, J. Wang, S. L. Gaw, K. Parida, P. S. Lee, *Adv. Energy Mater.* **2017**, *7*, 1701243.

[41] S. Jang, M. La, S. Cho, Y. Yun, J. H. Choi, Y. Ra, S. J. Park, D. Choi, *Nano Energy* **2020**, *70*, 104541.

[42] S. Jang, Y. Joung, H. Kim, S. Cho, Y. Ra, M. Kim, D. Ahn, Z.-H. Lin, D. Choi, *Nano Energy* **2022**, *97*, 107213.

This article is protected by copyright. All rights reserved.

Accepted Article

15214095, ja, Downloaded from https://onlinelibrary.wiley.com/doi/10.1002/adma.202308197 by Nanyang Technological University Lee Kong Chian School Of Medicine, Wiley Online Library on [16/10/2023]. See the Terms and Conditions (https://onlinelibrary.wiley.com/terms-and-conditions) on Wiley Online Library for rules of use; OA articles are governed by the applicable Creative Commons License

[43] D. Kam, G. Gwon, S. Jang, D. Yoo, S. J. Park, M. La, D. Choi, *Adv. Mater.* **2023**, *35*, 2303681.

[44] G. Shin, H. Yong, J. Chung, E. Cho, J. Ju, Z.-H. Lin, D. Kim, H. Lee, B. Koo, S. Lee, *Nano Energy* **2021**, *82*, 105713.

[45] D. Yoo, S. Jang, S. Cho, D. Choi, D. S. Kim, *Adv. Mater.* **2023**, *35*, 2300699.

[46] J. Chung, D. Heo, G. Shin, S.-H. Chung, J. Hong, S. Lee, *Nano Energy* **2021**, *82*, 105687.

[47] Q. Zhang, Q. Liang, Q. Liao, M. Ma, F. Gao, X. Zhao, Y. Song, L. Song, X. Xun, Y. Zhang, *Adv. Funct. Mater.* **2018**, *28*, 1803117.

[48] B. Kil Yun, H. Soo Kim, Y. Joon Ko, G. Murillo, J. Hoon Jung, *Nano Energy* **2017**, *36*, 233-240.

[49] X. Wei, B. Wang, X. Cao, H. Zhou, Z. Wu, Z. L. Wang, *Nat. Food* **2023**, *4*, 721-732.

[50] J. Peng, L. Zhang, W. Sun, Y. Liu, D. Yang, M. Feng, Y. Feng, D. Wang, *Appl. Mater. Today* **2022**, *29*, 101564.

[51] R. G. Neo, B. C. Khoo, *Appl. Energy* **2021**, *285*, 116428.

[52] R. K. Cheedarala, M. Shahriar, J. H. Ahn, J. Y. Hwang, K. K. Ahn, *Nano Energy* **2019**, *65*, 104017.

[53] S.-B. Jeon, D. Kim, M.-L. Seol, S.-J. Park, Y.-K. Choi, *Nano Energy* **2015**, *17*, 82-90.

[54] P. Jiang, L. Zhang, H. Guo, C. Chen, C. Wu, S. Zhang, Z. L. Wang, *Adv. Mater.* **2019**, *31*, 1902793.

[55] K. G. Marinova, R. G. Alargova, N. D. Denkov, O. D. Velev, D. N. Petsev, I. B. Ivanov, R. P. Borwankar, *Langmuir* **1996**, *12*, 2045-2051.

[56] X. J. Zhao, G. Zhu, Y. J. Fan, H. Y. Li, Z. L. Wang, *ACS Nano* **2015**, *9*, 7671-7677.

[57] B. Chen, Y. Yang, Z. L. Wang, *Adv. Energy Mater.* **2018**, *8*, 1702649.

[58] C. Zhang, Y. Liu, B. Zhang, O. Yang, W. Yuan, L. He, X. Wei, J. Wang, Z. L. Wang, *ACS Energy Lett.* **2021**, *6*, 1490-1499.

[59] S. Yong, H. Wang, Z. Lin, X. Li, B. Zhu, L. Yang, W. Ding, R. Liao, J. Wang, Z. L. Wang, *Adv. Energy Mater.* **2022**, *12*, 2202469.

[60] Y. Wang, D. Liu, Z. Hu, T. Chen, Z. Zhang, H. Wang, T. Du, S. L. Zhang, Z. Zhao, T. Zhou, M. Xu, *Adv. Mater. Technol.* **2021**, *6*, 2001270.

[61] S. Xu, Y. Feng, Y. Liu, Z. Wu, Z. Zhang, M. Feng, S. Zhang, G. Sun, D. Wang, *Nano Energy* **2021**, *85*, 106023.

This article is protected by copyright. All rights reserved.

Accepted Article

15214095, ja, Downloaded from https://onlinelibrary.wiley.com/doi/10.1002/adma.202308197 by Nanyang Technological University Lee Kong Chian School Of Medicine, Wiley Online Library on [16/10/2023]. See the Terms and Conditions (https://onlinelibrary.wiley.com/terms-and-conditions) on Wiley Online Library for rules of use; OA articles are governed by the applicable Creative Commons License

[62] M. R. Buchmeiser, *Angew. Chem. Int. Ed.* **2001**, *40*, 3795-3797.

[63] M. Seo, M. A. Amendt, M. A. Hillmyer, *Macromolecules* **2011**, *44*, 9310-9318.

[64] A.-H. Lu, F. Schüth, *Adv. Mater.* **2006**, *18*, 1793-1805.

[65] D. Wu, F. Xu, B. Sun, R. Fu, H. He, K. Matyjaszewski, *Chem. Rev.* **2012**, *112*, 3959-4015.

[66] T. Huang, Y. Long, Z. Dong, Q. Hua, J. Niu, X. Dai, J. Wang, J. Xiao, J. Zhai, W. Hu, *Adv. Sci.* **2022**, *9*, 2204519.

[67] T. He, Y. Zhang, Y. Chen, Z. Zhang, H. Wang, Y. Hu, M. Liu, C.-W. Pao, J.-L. Chen, L. Y. Chang, Z. Sun, J. Xiang, Y. Zhang, S. Chen, *J. Mater. Chem. A* **2019**, *7*, 20840-20846.

[68] T. Huang, Y. Long, B. Zhao, Q. Hua, Z. L. Wang, W. Hu, *ACS Appl. Mater. Interfaces* **2023**, *15*, 26682-26690.

[69] J. Wu, F. Xu, S. Li, P. Ma, X. Zhang, Q. Liu, R. Fu, D. Wu, *Adv. Mater.* **2019**, *31*, 1802922.

[70] S. Li, J. Nie, Y. Shi, X. Tao, F. Wang, J. Tian, S. Lin, X. Chen, Z. L. Wang, *Adv. Mater.* **2020**, *32*, 2001307.

[71] X. Zhang, Y. Dong, X. Xu, H. Qin, D. Wang, *Sci. China Technol. Sci.* **2022**, *65*, 282-292.

[72] C. Li, X. Liu, D. Yang, Z. Liu, *Nano Energy* **2022**, *95*, 106998.

[73] J. Chen, H. Guo, J. Zheng, Y. Huang, G. Liu, C. Hu, Z. L. Wang, *ACS Nano* **2016**, *10*, 8104-8112.

[74] S. Yun, S. Cho, H. W. Kim, S. B. Cho, S. Lee, K. Yong, *Nano Energy* **2022**, *103*, 107783.

[75] P. Wang, S. Zhang, L. Zhang, L. Wang, H. Xue, Z. L. Wang, *Nano Energy* **2020**, *72*, 104703.

[76] F. Wang, P. Yang, X. Tao, Y. Shi, S. Li, Z. Liu, X. Chen, Z. L. Wang, *ACS Nano* **2021**, *15*, 18206-18213.

[77] X. Zhao, X. Lu, Q. Zheng, L. Fang, L. Zheng, X. Chen, Z. L. Wang, *Nano Energy* **2021**, *87*, 106191.

[78] R. Zhang, H. Lin, Y. Pan, C. Li, Z. Yang, J. Tian, H. C. Shum, *Adv. Funct. Mater.* **2022**, *32*, 2208393.

[79] B. Fan, A. Bhattacharya, P. R. Bandaru, *Nat. Commun.* **2018**, *9*, 4050.

[80] W. Xu, X. Zhou, C. Hao, H. Zheng, Y. Liu, X. Yan, Z. Yang, M. Leung, X. C. Zeng, R. X. Xu, Z. Wang, *Nat. Sci. Rev.* **2019**, *6*, 540-550.

[81] Z. L. Wang, A. C. Wang, *Mater. Today* **2019**, *30*, 34-51.

This article is protected by copyright. All rights reserved.

Accepted Article

15214095, ja, Downloaded from https://onlinelibrary.wiley.com/doi/10.1002/adma.202308197 by Nanyang Technological University Lee Kong Chian School Of Medicine, Wiley Online Library on [16/10/2023]. See the Terms and Conditions (https://onlinelibrary.wiley.com/terms-and-conditions) on Wiley Online Library for rules of use; OA articles are governed by the applicable Creative Commons License

[82] S. Lin, L. Xu, C. Xu, X. Chen, A. C. Wang, B. Zhang, P. Lin, Y. Yang, H. Zhao, Z. L. Wang, *Adv. Mater.* **2019**, *31*, 1808197.

[83] C. Xu, Y. Zi, A. C. Wang, H. Zou, Y. Dai, X. He, P. Wang, Y.-C. Wang, P. Feng, D. Li, Z. L. Wang, *Adv. Mater.* **2018**, *30*, 1706790.

[84] J. You, J. Shao, Y. He, F. F. Yun, K. W. See, Z. L. Wang, X. Wang, *ACS Nano* **2021**, *15*, 8706-8714.

[85] L. Sun, Z. Wang, C. Li, W. Tang, Z. Wang, *Nanoenergy Adv.* **2023**, *3*, 1-11.

[86] S. Niu, S. Wang, L. Lin, Y. Liu, Y. S. Zhou, Y. Hu, Z. L. Wang, *Energy Environ. Sci.* **2013**, *6*, 3576-3583.

[87] Z. Ying, Y. Long, F. Yang, Y. Dong, J. Li, Z. Zhang, X. Wang, *Analyst* **2021**, *146*, 1656-1662.

[88] B. Zhang, L. Zhang, W. Deng, L. Jin, F. Chun, H. Pan, B. Gu, H. Zhang, Z. Lv, W. Yang, Z. L. Wang, *ACS Nano* **2017**, *11*, 7440-7446.

[89] K. Liu, Y. Zhou, F. Yuan, X. Mo, P. Yang, Q. Chen, J. Li, T. Ding, J. Zhou, *Angew. Chem. Int. Ed.* **2016**, *55*, 15864-15868.

[90] G. Chen, X. Liu, S. Li, M. Dong, D. Jiang, *Lab Chip* **2018**, *18*, 1026-1034.

[91] L. Ma, R. Wu, A. Patil, J. Yi, D. Liu, X. Fan, F. Sheng, Y. Zhang, S. Liu, S. Shen, J. Wang, Z. L. Wang, *Adv. Funct. Mater.* **2021**, *31*, 2102963.

This article is protected by copyright. All rights reserved.

Accepted Article

15214095, ja, Downloaded from https://onlinelibrary.wiley.com/doi/10.1002/adma.202308197 by Nanyang Technological University Lee Kong Chian School Of Medicine, Wiley Online Library on [16/10/2023]. See the Terms and Conditions (https://onlinelibrary.wiley.com/terms-and-conditions) on Wiley Online Library for rules of use; OA articles are governed by the applicable Creative Commons License

Accepted Article

Feng Jiang is a Ph.D. candidate at the School of Materials Science and Engineering, Nanyang Technological University. His current research interests focus on the design and fabrication of multifunctional composite-based energy harvesters and their applications in self-powered sensors and wearable electronics.

Liuxiang Zhan is a Ph.D. candidate in the College of Textiles, Donghua University. He is also a visiting graduate in the School of Materials Science and Engineering, Nanyang Technological University. His research focus on smart textiles, self-powered systems, wearable electronics and soft robotics.

This article is protected by copyright. All rights reserved.

15214095, ja, Downloaded from https://onlinelibrary.wiley.com/doi/10.1002/adma.202308197 by Nanyang Technological University Lee Kong Chian School Of Medicine, Wiley Online Library on [16/10/2023]. See the Terms and Conditions (https://onlinelibrary.wiley.com/terms-and-conditions) on Wiley Online Library for rules of use; OA articles are governed by the applicable Creative Commons License

Accepted Article

Jin Pyo Lee received his Ph.D. in material science and engineering at Ulsan National Institute of Science and Technology University in 2022. He is currently a research fellow at Nanyang Technological University, Singapore. His main research interests involve self-powered wearable/portable devices and human-machine interfaces application.

Pooi See Lee received her Ph.D. degree from National University of Singapore in 2002 in the field of semiconductor materials. She is currently the President's Chair Professor in Materials Science and Engineering at Nanyang Technological University, Singapore. Her current research focuses on soft electronics, mechanical energy harvesters, human-machine interfaces, sensors and actuators, wearable technology, and hybrid materials for soft robotics.

This article is protected by copyright. All rights reserved.

15214095, ja, Downloaded from https://onlinelibrary.wiley.com/doi/10.1002/adma.202308197 by Nanyang Technological University Lee Kong Chian School Of Medicine, Wiley Online Library on [16/10/2023]. See the Terms and Conditions (https://onlinelibrary.wiley.com/terms-and-conditions) on Wiley Online Library for rules of use; OA articles are governed by the applicable Creative Commons License

Accepted Article

WILEY-VCH

Fluid-based triboelectric nanogenerators (FB-TENGs) are emerging energy technologies with improved effective contact area and prolonged triboelectric effect compared to their solid-based counterparts. This review summarizes the working mechanism and optimization strategies of various FB-TENGs, including liquid-solid, gas-solid, liquid-liquid and gas-liquid TENGs. Their respective advantages, applications, and challenges, have been also systematically discussed, offering a guidance for designing high-performance FB-TENGs.

F. Jiang, L. Zhan, J. P. Lee, Prof. P. S. Lee *

Triboelectric Nanogenerators Based on Fluid Medium: From Fundamental Mechanisms toward Multifunctional Applications

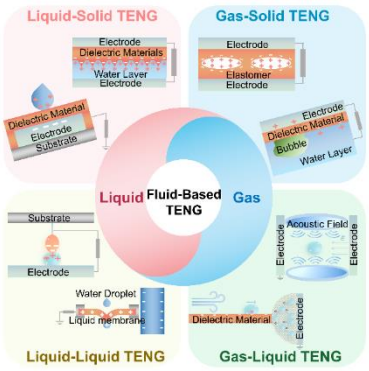

ToC figure

This article is protected by copyright. All rights reserved.

15214095, ja, Downloaded from https://onlinelibrary.wiley.com/doi/10.1002/adma.202308197 by Nanyang Technological University Lee Kong Chian School Of Medicine, Wiley Online Library on [16/10/2023]. See the Terms and Conditions (https://onlinelibrary.wiley.com/terms-and-conditions) on Wiley Online Library for rules of use; OA articles are governed by the applicable Creative Commons License